SCIENCE CHINA
Chemistry

•REVIEWS•

July 2021 Vol.64 No.7: 1131–1156
https://doi.org/10.1007/s11426-021-1011-9

High safety separators for rechargeable lithium batteries

Miaomiao Su[1†], Guang Huang[1†], Suqing Wang[1*], Yanjie Wang[3] & Haihui Wang[2*]

[1]*School of Chemistry and Chemical Engineering, South China University of Technology, Guangzhou 510640, China;*
[2]*Beijing Key Laboratory of Membrane Materials and Engineering, Department of Chemical Engineering, Tsinghua University, Beijing 100084, China;*
[3]*Shenzhen Senior Technology Material Co., Ltd., Shenzhen 518106, China*

Received January 21, 2021; accepted April 14, 2021; published online April 25, 2021

Lithium-ion batteries (LIBs) are presently dominant mobile power sources due to their high energy density, long lifespan, and low self-discharging rates. The safety of LIBs has been concerned all the time and become the main problem restricting the development of high energy density LIBs. As a significant part of LIBs, the properties of separators have a significant effect on the capacity and performances of batteries and play an important role in the safety of LIBs. In recent years, researchers devoted themselves to the development of various multi-functional safe separators from different views of methods, materials, and practical requirements. In this review, we mainly focus on the recent progress in the development of high-safety separators with high thermal stability, good lithium dendritic resistance, high mechanical strength and novel multifunction for high-safety LIBs and have in-depth discussions regarding the separator's significant contribution to enhance the safety and performances of the batteries. Furthermore, the future directions and challenges of separators for the next-generation high-safety and high energy density rechargeable lithium batteries are also provided.

separator, high safety, lithium-ion batteries

Citation: Su M, Huang G, Wang S, Wang Y, Wang H. High safety separators for rechargeable lithium batteries. *Sci China Chem*, 2021, 64: 1131–1156, https://doi.org/10.1007/s11426-021-1011-9

1 Introduction

With the shortage of fossil fuel resources and the increasingly serious environmental and ecological problems, people have begun to pursue cleaner and more environmentally-friendly energy. Lithium-ion batteries (LIBs) have attracted more and more attention because of their high energy density and power density. Nowadays, LIBs are widely used in our daily-life, such as electric vehicles, laptops and digital cameras. There is no doubt that LIBs play an important role in our lives and productivity and become an indispensable part of our lives.

However, there are serious safety risks during the working process of batteries. This unsafe behavior mainly stems from its thermal runaway [1,2], which usually causes fire or serious explosion accidents. It is confirmed that there are a series of potential exothermic side reactions in LIBs, such as the thermal decomposition of solid-electrolyte interphase (SEI) films, the further exothermic reactions between fresh lithium and electrolytes, the thermal decomposition of electrolytes and cathode materials. When the battery works in abuse conditions such as short circuit, overcharge, overheating, or high rate charge, a large amount of heat is released in a short time, the internal temperature will increase, and these exothermic side effects will be triggered successively [3]. Once the heat is unable to dissipate quickly, the battery would lead to continuous temperature rise, resulting in the combustion or even an explosion [4]. Meanwhile, there are many causes for the thermal runaway, among which in-

†These authors contributed equally to this work.
*Corresponding authors (email: cesqwang@scut.edu.cn; cehhwang@tsinghua.edu.cn)

ternal short-circuits are the predominant reason. During this process, the separator usually undergoes a series of obvious changes, such as the blocking of pores, thermal shrinkage caused by internal temperature rise, puncture caused by external impact and uncontrollable dendrite growth.

Based on the above problems, great efforts have been made for improving each component of the battery [5–7]. One of the fundamental and effective methods to solve the safety issues of batteries is to develop a high-performing separator. As a significant component of a battery, the separator may play different roles in different battery systems [8–11]. In LIBs, the separator is placed between the positive and negative electrodes to prevent the two electrodes from short-circuiting upon contact. The properties of separators are correlated with the safety and electrochemical performances of LIBs. The research about separators have attracted much attention, and the publications are increasing during the past 10 years. The unique term of "separator" and "lithium" appears in the titles, abstracts, and/or keywords of >4,500 publications, with a clearly increase of the field as a function of published papers per year (Figure 1(a)). Naturally, a fine collection of reviews mostly described the impact of separator properties on the LIB from the material, the preparation method, and the separator used in different battery systems (lithium–sulfur batteries, lithium–air batteries, *etc*.). With the development of high energy density LIBs, the research on the design of high-safety separators has been emerging, and it is necessary to summarize the research progress of safety separators in recent years, especially in the last five years. In addition to the research, the global market demand of separators for LIBs shows fast-growing in the aspect of industry with the rapid development of electric vehicles (Figure 1(b)). The shipment of separators for LIBs greatly increases to 37.2×10^8 m^2 in China in 2020 which is 4.8 times as much as that in 2015 (7.7×10^8 m^2). The fast-growing separator market and the increased demand for high-safety LIBs also promote the research interest of high-performance separators.

In this review, we summarize the development direction and research progress of high-safety batteries in recent years. In particular, the recent progress of thermally stable separators, lithium dendrite-proof separators, separators with high mechanical stability, and other novel multi-functional separators is discussed in detail. Finally, the challenges and future perspectives of high-safety separators are discussed.

2 Characteristics and requirements of separators for LIBs

The basic requirements of separators should be inert during charge/discharge process of batteries and served as a medium to allow lithium ion transport. In terms of safety application of LIBs, a separator should have the following major characteristics: excellent chemical/electrochemical stability, good thermal resistance, high mechanical strength, and dendrite resistance. Secondly, considering that, in practical applications, the potential risks inside the battery are often unable to be monitored and prevented in time, constructing a self-protection and intelligent response separator can reduce the risk factors and alleviate hazards.

In practical applications, the high chemical and electrochemical stability of separators are of great significance to the safe operation of the battery. It requires the separator to be inert to the electrolyte and electrode materials during battery cycling process.

Separators should have a proper thickness in order to reduce the internal resistance of the battery and increase the energy and power density of the battery, under the premise of ensuring a certain mechanical strength. In addition, the uniform thickness of the battery separator is also an important indicator of battery consistency, which has a great impact on battery performances.

Good electrolyte wettability is conducive to the affinity between the separator and the electrolyte, thereby increasing the ion conductivity and improving the electrochemical performance of LIBs. However, poor wettability of separators is not conducive to the uniform transmission of lithium ions, which will cause the generation of lithium dendrites and threaten the safe operation of the battery. The electrolyte wettability is correlated to the porosity, pore structure and surface properties of the separator.

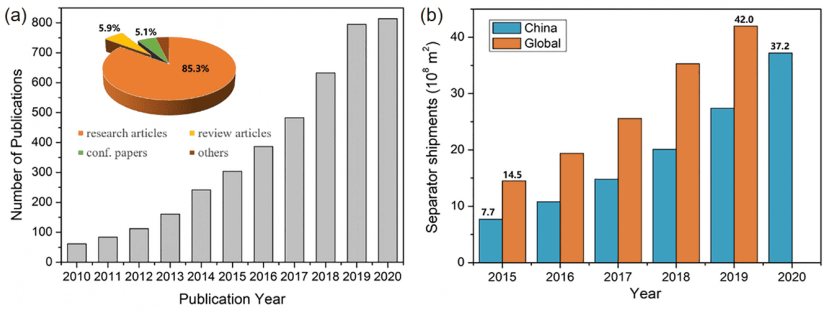

Figure 1 (a) Publications growth of "separator" and "lithium" based on Web of Science database (excluding patents); (b) Shipments growth of separators for LIBs in China and global markets (color online).

Proper porosity is very important for improving electrolyte wettability and absorption. Low porosity will result in low electrolyte absorption and large internal resistance of the battery, which is not conducive to the transport of lithium ions. However, too high porosity might poison the mechanical strength of the separator. Generally, the ideal separator porosity should be 40%–60%. The ratio of pore volume to apparent geometric volume is considered as the porosity. The pore size and distribution of separators have a significant impact on battery's performances. The separator with too large pore size is likely to cause a short circuit due to direct contact between the positive and negative electrodes or easily pierced by lithium dendrites, which is not conducive to the safety of the battery, while too small pore size will increase the internal resistance. Generally, the pore size of the ordinary battery separator should be sub-micron level (<1 μm). In addition, the uniform pore size distribution of separators could facilitate the uniform ion transport, ensure consistent electrode/electrolyte interface properties, reduce the generation of lithium dendrites, and then improve the safety of the battery.

Thermal stability and thermal shutdown of separators are directly correlated to the safety of the batteries. When the battery is short-circuited or overcharged, a large amount of heat will be released, resulting in heat accumulation and temperature rise. Therefore, when the temperature rises, the separator should maintain the original integrity and certain mechanical strength to block the positive and negative electrodes to prevent short circuits. As a basic requirement, the thermal shrinkage of the separator is less than 5% after 1 h at 100 °C [12]. When overheating or short circuit occurs, the ability to block the pores in time to shut down the battery is essential. More importantly, when the pores are closing, the separator should still have a certain degree of mechanical integrity to ensure the separation of cathodes and anodes to reduce thermal runaway.

The mechanical properties of the separator are also very important. The mechanical properties of the separator are characterized by tensile strength and puncture strength. A qualified separator should have high tensile strength (>1,000 kg cm^{-1}) and puncture strength (>300 g mil^{-1}) to cope with the stress generated during battery assembly and withstand the penetration of lithium dendrites during the battery cycling [13]. Generally, a thicker separator has the better mechanical strength which has stronger puncture resistance. However, the internal resistance also increases with the increase of thickness, which highly affects the performance of LIBs.

Accelerating rate calorimeter (ARC-ES, THT) test aims to study the temperature-responsive behaviours of the coin cells using different separators in the case of adiabatic short-circuiting. The thermal shutdown temperature and sluggish thermal-responsive rate can evaluate whether the separator can control the temperature rise well or not [14]. Important mechanical properties include the tensile strength and Young's modulus. The tensile strength including elongation at breakage and Young's modulus can be deduced from the strain rate-dependent stress–strain curves with an electronic universal testing instrument. Different from the Young's modulus evaluated by tensile strength, the surface Young's modulus of the separator measured by atomic force microscopy (AFM) in the peak-force quantitative nano-mechanics mode can determine whether the tough surface can effectively suppress the dendritic Li growth or not [15,16]. Dynamic mechanical thermal analysis (DMA) and thermal mechanical analysis (TMA) are used to evaluate the variation trend of mechanical strength at different directions during the heating process [17].

The process of lithium-ion migration and electrochemical deposition in the battery is still an open topic of research, which will undoubtedly benefit from the advances in characterizations and simulations. Mathematical modelling and numerical simulation are widely used to help deepen the understanding of electrochemical systems and ion migration. COMSOL simulations highlight the impact of ionic conductivity and the transference number on battery's performances by simulating the electrolyte salt concentration and electrolyte potential as function of distance across the separator in a symmetric Li *vs.* Li cell, the separator's structure and the interaction between electrolyte and separator surface [18]. In addition, the corresponding model of Li ion concentration distribution, the lithium dendrites growth speed and the performance of separators can be compared [15,19]. By virtue of the commercial software ABAQUS, finite element calculation can be realized easily. For example, the interaction between an elastic piercing tip and curved/planar substrates using two-dimensional (2D) nonlinear finite element method can be simulated. According to the distribution of stress intensity, the interaction between the lithium dendrites and ceramic coating layers can be determined [19].

3 The design of high-safety separators

The safety of batteries has always attracted people's attention and becomes more and more important due to the demand for high energy density batteries [20]. Based on the function of separators in LIBs, the properties of separators directly influence the reliability (including safety and electrochemical performances) of the LIBs. The thermal runaway process in the battery, which starts from the overheating of the battery, is the root cause of fires and explosions of the battery. In the early stages of thermal runaway, metal fragments from collisions and lithium dendrites from the battery cycle may puncture the separator, causing internal short circuit and

triggering a large current which will generate large amount of heat, causing a series of exothermal side reactions between electrodes and electrolytes, and contribute to the continue rise in temperature, leading to more serious thermal shrinkage of the separator and thus more serious short-circuiting. In the late period of thermal runaway, oxygen and heat accumulate continuously, and the combustible electrolyte will burn out of control, eventually causing fire and explosion. Along this line of reactions, separators and electrolytes play important role in the thermal runaway process. In the separator part, it is critical to design the advanced separators with high thermal stability, lithium dendrites-proof properties, mechanical stability and novel multi-functions to improve the safety of LIBs.

However, current commercial polyolefin separators such as polyethylene (PE) and polypropylene (PP) with low melting points could not sustain their dimension at elevated temperature, leading to internal short circuit and safety risk in the LIBs. The polyolefin separators also exhibit poor electrolyte wettability due to the low porosity and low polarity which might lead to inhomogeneous lithium ion transport and serious dendrites. The generation of lithium dendrites will destroy the generated SEI layer and continue to react with the electrolyte to form a new SEI film, resulting in the constant consumption of electrolytes and the formation of dead lithium, which will eventually increase interface resistance and lower the reversible capacity of LIBs [21]. The high mechanical strength of the separator is very important to improve the safety of LIBs. A qualified separator needs to maintain good mechanical integrity after it is subjected to the harm such as stress generated during battery assembly, damage caused by collisions and falling, and puncture of lithium dendrites during cycling, for which the mechanical damage of the separator will cause the internal short circuit and may lead to the ultimate failure of the LIBs. With the development of LIBs, several novel separators with multi-functions such as intelligent response separators (*e.g.* hot shutdown, dendrite warning) and flame-retardant separators are gradually developed. With the above analysis, it is critical to design the advanced separator to meet the requirements of advanced LIBs.

3.1 Thermally stable separators

As we all know, a safe separator should have high dimensional stability at elevated temperature. Although polyolefin separators offer excellent mechanical strength and chemical stability, they have a low melting point (PE/130 °C, PP/165 °C) and exhibit obvious shrinkage at elevated temperature and cannot guarantee the safety of the battery under extreme conditions. It was reported that functionalized polyolefin separators with thermally stable coating layers can improve the thermal resistance property [22,23]. In recent years, researchers have made significant progress in the research of modified and new separators, but the commercial applications are still in the range of PE or PP based polyolefin membranes and ceramic-modified polyolefin separators. The main limitation is cost, such as the cost of raw materials and the manufacturing process. However, limited by the characteristics of polyolefin materials, the modified polyolefin separators are difficult to be stable at higher temperatures (>200 °C). For some special applications with higher requirements, high thermal stable separators with a high heat-resistant skeleton are expected to be used commercially due to their excellent performance. Since the growing demand for high energy density batteries, the thinner and lighter coating layer is really needed in addition to good thermal stability. Furthermore, various non-woven mats with high heat-resistant skeletons have also been explored to replace polyolefin as safer separators.

3.1.1 Inorganic ceramic coated separators

Benefiting from the high heat-resistance of inorganic particles, the introduction of ceramic coatings into polyolefin membranes is an effective means to improve the thermal stability of the separators. Traditional inorganic-coating separators often use hydrophilic polymers as binders, and Al_2O_3, ZrO_2, SiO_2, zeolite and other ceramic particle coatings are introduced on the surface of the polyolefin substrate [24–31]. It is proved that the ceramic-coating separators have enhanced thermal stability, good wettability and high uptake of liquid electrolytes, which greatly improves the safety and cycle stability of the battery. Yang *et al*. [32] synthesized core–shell structured silica–poly(methyl methacrylate) (SiO_2–PMMA) sub-microspheres and coated them on one side of a PE separator to fabricate a functional ceramic-coated separator (FCC separator). The heat-resistant SiO_2 core particle layers suppressed the more thermal shrinkage (12.9%) than that in the PE separator (31.4%) at 130 °C for 30 min. Cho *et al*. [27] used amino-functionalized SiO_2 (N-SiO_2) particles to coat both sides of polyethylene separators. Due to the incorporation of hydrophilic amino groups and the thermally-resistant N-SiO_2, the composite separator had good affinity for polar solvents and showed only 10% thermal shrinkage at 150 °C. Boateng *et al*. [33] selected acetone as a solvent for the large zeta-potential (ζ) with the powders. And the results showed that SiO_2 nanoparticles had a good suspension stability and dispersity in acetone.

However, many ceramic-coating separators still exhibited the poor thermal stability due to the low melting point of common polymer binders, such as polyvinylidene fluoride-hexafluoropropylene (PVDF–HFP), PMMA and PVDF [15,32]. Once the binder reaches the molten state, the bonding force between the coating and the separator may be weakened or even the ceramic particles would disperse unevenly in the melted polymer binder, which is not conducive

to the heat resistance of the coating. In order to ensure the safety of batteries at high temperatures, substituting high melting-point polymers for traditional binders is an effective strategy [34]. Shi *et al*. [35] studied an Al_2O_3 coating separator (CCS–PI) with the thickness of 6 μm bonded by a high thermally-stable polyimide (PI) binder (sustain thermal stability at temperature even up to 500 °C) onto the surface of PE porous membranes. The adhesion strength between the PE separator and the ceramic coating layer with PI binders (1.2 MPa) was higher than that between the PE separator and the ceramic coating layer using PVDF–HFP binders (0.5 MPa). The CCS–PI showed no thermal shrinkage at up to 160 °C and remained stable when it is packed in the batteries at up to 165 °C. Furthermore, Dai *et al*. [36] proposed a rational design involving a PDA-SiO_2 composite-modified PE separator by a simple dip-coating. The PDA formed an overall-covered self-supporting film throughout ceramic layers and the pristine PE separator, which made the ceramic layer and the PE separator appeared as a whole aspect. As a result, the developed composite-modified separator displayed highly enhanced thermal and mechanical stability, showing no obvious shrinkage at 220 °C compared with the PE-SiO_2 separator (shrinkage of 28.4% at 170 °C).

Most of the slurries above used for coating modification were dispersed by organic solvents. Because the toxic organic solvents tend to pollute the environment and increase the cost of organic solvent recovery, many environmentally-friendly strategies using water-based ceramic slurries were developed by adding surfactants or water-soluble polymeric binders like sodium alginate (SA), polyvinyl alcohol (PVA), carboxymethyl cellulose sodium (CMC) [37]. Yang *et al*. [38] reported a separator made by coating boehmite (AlOOH) particles with PVA on microporous PE membranes. On account of the excellent adhesion and film-forming properties of the binder PVA, an inter-locking interface structure was formed between the PE film and the AlOOH coating, which greatly enhanced the thermal stability of the modified separator (the thermal shrinkage rate is less than 3% after exposure at 180 °C for 0.5 h). Jeon *et al*. [24] developed a water-based ceramic coating method using a surfactant and a water-soluble polymeric binder CMC. This process was economic and environmentally-friendly, and diminished the poor affinity between the non-polar solvent and the hydrophilic Al_2O_3 particles.

Apart from the above problems, the thickness and weight of ceramic coated separators obtained by a blade-coating process increases significantly, which may reduce the ion conductivity and the energy density of LIBs. So, how to design a thinner and lighter separator with high thermal stability in a simple way is still a research hotspot. The representative surface modified separator for LIBs and their basic properties were summarized in Table 1.

Table 1 Summaries of surface modified polyolefin separators for LIBs

Materials	Thickness [a)–c)] (μm)	Mass loading (mg cm^{-2})	Porosity (%)	Thermal shrinkage (%)	Ionic conductivity (mS cm^{-1})	Ref.
LLZTO	PP+5	0.9	–	–	–	[15]
PE–Al_2O_3	PE_1+6	–	–	0% at 140 °C for 0.5 h	0.846	[24]
N–SiO_2	PE_1+5	–	–	10% at 150 °C for 0.5 h	0.81	[27]
LiAl LDH@PP	PP+19	–	–	–	–	[28]
FCC	PE_1+5	–	–	12.9% at 130 °C for 0.5 h	1.08	[32]
CCS–PI	PE_1+6	–	–	0% at 140 °C for 0.5 h	0.70	[35]
PE–SiO_2@PDA	PE_1+6	–	44.1	0% at 220 °C for 0.5 h	0.981	[36]
AlOOH	PE_2+1.15	–	–	<3% at 180 °C for 0.5 h	6.56	[38]
LSO–SiO_2@PE	PE_3+3	–	–	0% at 150 °C for 0.5 h	0.41	[39]
PVDF–HFP/colloidal–TiO_2	PP+15	–	57	4.8% at 150 °C for 1 h	0.49	[40]
PE–BN/PVDF–HFP	40	–	50.8	6.6% at 140 °C for 1 h	0.44	[41]
TiO_2–Kynar	–	1.8	–	36% at 160 °C for 1 h	–	[42]
APP@SiO_2	PP+40	–	50.91	0% at 180 °C for 0.5 h	0.84	[43]
CCS	PE_1+3	–	–	29.3% at 145 °C for 0.5 h	1.12	[44]
ST	PE_1+9	–	–	18.95% at 150°C for 0.5 h	0.82	[45]
ATP–PVA	PE_1+4	–	45.8	0% at 170 °C for 0.5 h	0.782	[46]
MBO@PP	PP+6	0.346	–	–	0.98	[47]
BS–Al_2O_3@PE	PE_2+8	–	–	0% at 200 °C for 0.5 h	0.683	[48]

a) The thickness of PP is 25 μm. b) The thickness of PE_1 is 20 μm. c) The thickness of PE_2 and PE_3 are 16 μm and 12 μm, respectively.

3.1.2 Ultrathin modified separators

According to practical applications, thinner separators can avoid occupying limited space inside the battery and thereby increase the energy density and power density of the battery to a certain extent. Up to now, various surface modification methods, such as ultraviolet (UV) or electron bean irradiation, plasma treatment, polydopamine (PDA) modification and coupling agent treatment, have been developed well because coating a nanometer scale layer on the membranes or particles can improve the affinity to the electrolyte and ensure the well-preserved original structure [22,49–53].

Moon *et al*. [54] prepared ultrathin Al_2O_3 coating layers by atomic layer deposition (ALD) and dopamine treatment (Figure 2(a)). By means of the hydrogen bonding between catechol and amine groups in PDA and the aluminium oxides that were terminated with hydroxyl groups, PE/Al_2O_3/PDA separators showed high thermal stability at 140 °C. Despite these advantages, the complex operation conditions and high cost compared with ceramic-coated separators may limit their further applications. Pan *et al*. [55] prepared a thin, thermally stable and low-cost nanocellulose layer through a simple filtration method, and laminated it on both sides of the plasma-treated PE film. Thanks to the hydrogen bonding between the nanocellulose layer and the plasma-treated PE film, the coating had a strong bonding force with the PE substrate, and thereby the modified separator still maintained good dimensional integrity at 200 °C. Dip-coating is another simple and powerful method to prepare multi-layer films and the driving forces that facilitate the layer-by-layer (LBL) self-assembly include electrostatic attraction, hydrogen-bond formation, covalent-bond formation, charge-transfer complex formation and other interactions [56,57]. Chi *et al*. [52] designed a ZrO_2/POSS multilayer deposited on PE separators by the LBL process, and the ZrO_2/POSS multilayer could decrease the number of EC molecules interacting with Li^+ and improve the mobility of solvated Li^+ relative to PF_6^-. Yuan *et al*. [58] adopted a similar approach to design a unique activating polymer multi-layer PEI(PAA/PEO)$_3$ on the surface of PE separators based on the hydrogen bonding force between PAA and PEO. The thickness of an assembled monolayer was typically several nanometers and the original pore structure maintained well.

In addition, special treatments like dopamine (PDA) and coupling agent modification can effectively increase the affinity between organic and inorganic compounds. Qiu *et al*. [48] designed a Si–O–B thin layer on the Al_2O_3-coated polyethylene separator by surface engineering (Figure 2(b)). This process not only constructed the hybrid three-dimensional network of Si–O–Si and Si–O–B, but also introduced effective Lewis acid and Brønsted acid sites, which could effectively trap anions by electrical charge attraction. The BS–Al_2O_3@PE separator presented the highest ionic conductivity and did not show obvious thermal shrinkage even at 200 °C. Na *et al*. [59] recently designed a separator *via* UVO plasma treatment, followed by silane hybridization that yielded a polymeric binder-free, thin SiO_2 nanoparticles-coating layer on the separator (Figure 2(c)). Coupling agents contributed to forming an orthogonal chemical bonding of silica NPs onto the PE separator and between silica NPs without sacrificing ionic conductivity and cell performances, and the chemical grafting of SiO_2 NPs provided strong adhesive strength, thermal shrinkage resistance partly.

Most of the above-mentioned strategies introduced functional groups on the surface through special treatments and controlled the thickness of the coating at the molecular level to achieve thinner and lighter coating layers. However, those processes (such as irradiation grafting) require some expensive special equipment, and these technologies also consume a mass of energy, which leads to an increase in the cost of the production process. In addition, the high radiant energy pre-treatment may cause a severe decrease in mechanical strength and damage the polymer matrix of the original separator. These problems and challenges limit their scale production and practical applications.

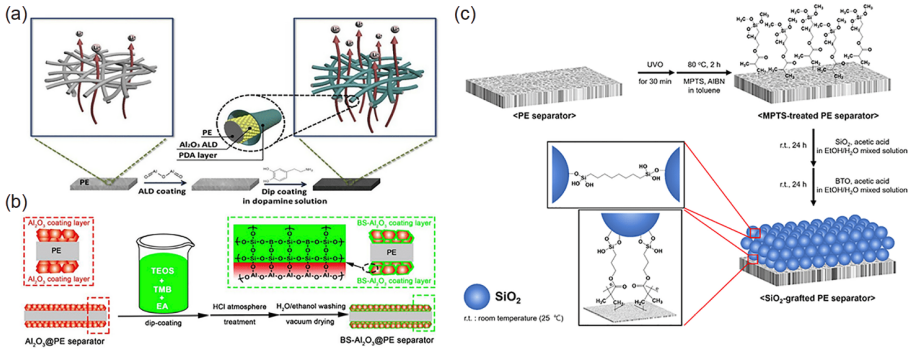

Figure 2 Schematic illustration of the preparation of the PE/Al_2O_3/PDA separator *via* atomic layer deposition and PDA treatment. (b) Schematic illustration for the preparation of BS–Al_2O_3@PE separator. (c) Schematic depiction of the fabrication of the SiO_2-grafted PE separator. (a) Reprinted with permission from Ref. [54], Copyright 2019, Elsevier. (b) Reprinted with permission from Ref. [48], Copyright 2020, Elsevier. (c) Reprinted with permission from Ref. [59], Copyright 2019, Elsevier (color online).

3.1.3 *Separators with high heat-resistant skeleton*

In addition to the surface coating strategy to enhance the thermal stability of the polyolefin separators, extensive efforts have been made to fabricate separators with high heat-resistant skeleton as high thermally-stable separators. As summarized in Table 2, various high heat-resistant separators based on polymers with high melting-point such as PVDF, PI, polybenzimidazole (PBI), polyacrylonitrile (PAN), poly-*p*-phenylene terephthamide (PPTA), polyurethane (PU), poly (*p*-phenylene benzobisoxazole (PBO) cellulose-based polymers and inorganic additives, have been explored to replace traditional porous polyolefin separators [37,60–71].

As a promising and efficient technique to produce non-woven nanofiber separators with high porosity, three-dimensional network structure and high surface area, electrospinning technology has obtained extensive attention [72]. PVDF, PAN, PET and PI are the most commonly reported single polymers to prepare monolayer electrospun separators due to their good electrochemical stability and excellent affinity of lithium ions [73–75]. Hao *et al*. [76] reported a PET separator with an average pore diameter of about 330 nm and high porosity (89%). Such a three-dimensional porous network structure enabled to adsorb a large amount of liquid electrolytes. Owing to the polar oxygen atoms and the carbon-oxygen double bond in polyetheretherketone (PEEK) which may interact strongly with the carbonate electrolytes, the PEEK-based separators are expected to have high thermal stability and good electrolyte wettability. Nevertheless, the weakness of poor solubility in organic solvents of PEEK limits its application [77]. To this end, Li *et al*. [75] in-

Table 2 Summaries of separators with high heat-resistant skeleton for LIBs

Materials	Methods	Thickness (μm)	Porosity (%)	Thermal shrinkage (%)	Ionic conductivity (mS cm^{-1})	Ref.
SA/ATP	Phase-inversion	20	–	0% at 250 °C for 2 h	1.15	[37]
CGC	Filtration	20	66	0% at 200 °C for 30 s	1.14	[53]
PVDF–PET	Electrospinning	12	80	0% at 135 °C for 1 h	–	[60]
PVDF/CMM/ZSM-5	Electrospinning	–	80	0% at 150°C for 1 h	1.72	[61]
PAN/SiO_2	Electrospinning	65	77	0% at 150 °C for 0.5 h	2.60	[62]
PPTA@PPS	Electrospinning	27–40	–	0% at 200 °C for 1 h	–	[64]
PU@GO	Electrospinning	100	90.7	20% at 170 °C for 1 h	3.73	[65]
Cellulose/PVDF–HFP	Phase-inversion	115	85.3	0% at 200 °C for 1 h	1.89	[66]
Cellulose/PVDF–HFP	Electrospinning	–	66.36	0% at 200 °C for 1 h	6.16	[67]
PBI/PI	Electrospinning	15	76–84	0% at 300 °C for 1 h	1.70–3.24	[74]
PEEK	Electrospinning	30	88	0% at 150 °C for 0.5 h	3.81	[75]
PET	Electrospinning	40	89	–	2.27	[76]
FPI	Electrospinning	35	73.4	–	1.14	[78]
PEI	Electrospinning	45	84.5	0% at 150 °C for 1 h	3.41	[79]
PMIA/OPS	Electrospinning	30–45	92.87	0% at 240 °C for 1 h	1.52	[82]
PVDF–HFP–PDA	Electrospinning	40	72.8	<15% at 170 °C for 0.5 h	1.40	[83]
PMIA@PVDF	Electrospinning	45	72.9	0% at 180 °C for 2 h	1.70	[85]
SNs	Filtration	~90	73	0% at 170 °C for 1 h	2.71	[86]
ECM	Filtration	12	59	0% at 160 °C for 2 h	0.26	[87]
Al_2O_3	Filtration	~50	–	0% at 150 °C for 1 h	1.70	[89]
CCN	Filtration	~12	50	–	0.45	[90]
PVDF	Electrospinning	–	80.3	–	1.35	[91]
PAN	Electrospinning	250	–	–	0.017	[92]
TiO_2@PI/PVDF–HFP	Electrospinning	–	87	0% at 180 °C for 0.5 h	2.36	[93]
SiO_2–PEI–PU	Electrospinning	50	83.57	3% at 170 °C for 0.5 h	3.33	[94]
PVP@TiO_2	Electrospinning	76	71	0% at 180 °C for 1 h	1.41	[95]
EMP	Electrospinning	60	–	0% at 200 °C for 1 h	1.70	[96]
h–BN	Phase-inversion	25–30	59	0% at 150 °C for 5 min	0.95	[97]
DVB–4VP	Phase-inversion	30	43	–	–	[98]
PVDF–HFP–ZrO_2	Phase-inversion	30	78.38	0% at 170 °C for 2 h	0.32	[99]
CLN/PPS	–	–	65	0% at 200 °C for 0.5 h	0.52	[100]

troduced polar functional groups (*e.g.*, carbonyl) and a rigid structure (*e.g.*, fluorenyl) into the molecular chains of the PEEK derivative to improve its solubility and thermal stability, and the obtain PEEK separators synthesized by electrospinning showed no shrinkage at 150 °C.

However, those electrospun non-woven separators usually showed poor mechanical properties. Mechanical press or heat treatment were often used to enhance physical properties and dimensional stability of the monolayer separator synthesized by electrospinning, which would be described in detail in a later section [78,79]. Besides, the introduction of the second component such as polymers or inorganic fillers is another effective method to improve the performance of monolayer membranes and has been widely studied [80]. Wang *et al*. [81] prepared electrospun PI–SiO_2 membranes by mixing SiO_2 into the polyamic acid (PAA) precursor solution and studied their performances. The introduction of SiO_2 nanoparticles improved the ionic conductivity of separators from 1.71 to 2.27 mS cm^{-1} as well as increased the maximum tensile stress (4.66 MPa), which is higher than that of PI membranes (3.77 MPa). Besides, slight amounts of SiO_2 nanoparticles tightly embedded in the polymide nanofibers with negligible thickness and weight increased, and the PI and PI-SiO_2 membranes simultaneously maintained an outstanding thermal stability at 250 °C (Figure 3(a–d)). Zhao *et al*. [82] reported a hybridpoly-*m*-phenyleneisophthalamide/octaphenyl-polyhedral oligomeric silsesquioxane (PMIA/octaphenyl-POSS) membrane (HPPS) with well thermal stability at 240 °C by the electrospinning technique. The organic-inorganic featured octaphenyl-POSS (OPS) endowed admirable compatibility of membrane matrix and the robust mechanical strength (21.79 MPa).

Coaxial electrospinning apparatus and dip-coating method can fabricate core-shell structured monolayer membranes [83–85]. Wang *et al*. [85] synthesized a core-shell structured PMIA@PVDF nanofiber membrane *via* coaxial electrospinning. The PMIA core strengthened the thermal stability and integrity of the whole separator. Meanwhile, the lyophilic PVDF shell guaranteed the membrane wettability to electrolytes and the ion conductivity. The PMIA@PVDF showed slight dimensional shrinkage compared to pure PVDF (melted completely at 220 °C) and improved the ionic conductivity from 1.2 to 1.7 mS cm^{-1}. Shi *et al*. [83] grew a thin PDA layer on the surface of PVDF–HFP nanofibers to form the unique core-shell structure by dip-coating. Due to the strong bonding between PVDF–HFP fibers and the coating layer by PDA, the PVDF–HFP–PDA composite membrane almost did not present bending or deformation at 160 °C and the tensile properties significantly improved from 7.1 to 11.2 MPa in the dry state and 3.5 to 7.1 MPa in the wet state, respectively. The design of the multilayer membrane to improve the mechanical strength of the separators and to enhance the intelligent protection of the battery will be described in detail in the next chapter.

Phase inversion is another commonly used method to obtain porous separators that meet the various requirements in different secondary battery systems [88]. In the phase inversion process, the solvent/non-solvent exchange occurs

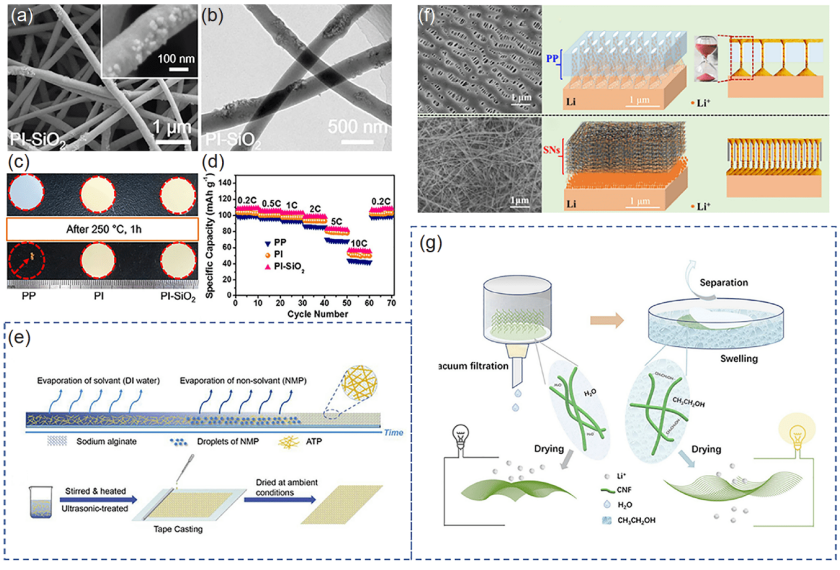

Figure 3 (a) Surface SEM images of PI–SiO_2 (the inset is corresponding high-magnification image); (b) TEM image of PI–SiO_2 nanofibers. (c) Thermal shrinkage after exposure at 250 °C for 1 h. (d) Electrochemical behaviors of $LiMn_2O_4$/Li cells: rate capabilities with PP, PI and PI–SiO_2 separators (0.2–10 C). (e) Schematic illustration of phase inversion method and overall procedure of the material preparation. (f) Schematic highlighting the distinct nature of Li deposition within the lithium-metal batteries using PP and SiO_2 nanowire (SN) membranes as separators. (g) Schematic illustration of the preparation of the cellulose nanofibril membrane. (a–d) Reprinted with permission from Ref. [81], Copyright 2017, Elsevier. (e) Reprinted with permission from Ref. [37], Copyright 2019, Elsevier. (f) Reprinted with permission from Ref. [86], Copyright 2019, American Chemical Society. (g) Reprinted with permission from Ref. [87], Copyright 2020, Elsevier (color online).

when casting polymer solution exposes to non-solvent environment, resulting in the formation of porous structures. Song and co-workers [37] fabricated a porous separator by incorporating attapulgite (ATP) nanofibers into sodium alginate (SA) (Figure 3(c)). With increasing the ATP content ratio in the solution, the ionic conductivity of the SA/ATP separator also increased from 0.49 to 1.15 mS cm^{-1} and the SA/ATP separator showed thermal stability (no shrinkage at 250 °C). Asghar *et al*. [66] prepared a porous and honeycomb-structured cellulose/PVDF–HFP membrane by using glycerol as a pore forming agent. The obtained cellulose/PVDF-HFP separator enabled large electrolyte uptake (310%), high lithium-ion transference number (0.89) and excellent thermal stability which could maintain the structure integrity even at 200 °C.

Vacuum filtration is often used to produce nanofibers-based separators. For example, Du *et al*. [86] designed a novel separator built with ultralong SiO_2 nanowires (SNs) by vacuum filtration (Figure 3(f)). Due to the characteristics of inorganic ceramics, the SNs separator could maintain its original shape even at 170 °C. He *et al*. [89] reported a pure ceramic separator made of Al_2O_3 nanowires, which offered high wettability, thermal stability, and exceptional electrochemical performances. A cellulose-based membrane could be a promising LIB separator for its super-thermal stability, hydrophilic property and environmental-friendliness. However, on account of the intensive hydrogen bonding of hydroxyl groups among nanocellulose, direct self-assembly of nanofibers by a filtration method resulted in a dense and nonporous membrane with very low ionic conductivity. Meanwhile, the concentration of the nanocellulose dispersion was usually no more than 1 wt.%, which limited the preparation method of nano-fibril membranes. Hence, many researchers improved the ionic conductivity by grafting functional groups or introducing pore-making agents [90]. Sheng and co-works [87] used a facile ethanol-soaked process to fabricate ultra-light (7.1 g m^{-2}) and ultra-thin (12 μm) cellulose nano-fibril membranes for LIBs (Figure 3(g)). The ethanol acted as a separating agent and replaced the water between the fibres, making the fibres looser and more porous with highly improved ionic conductivity and high thermal stability (no dimensional change at 160 °C for 2 h).

In contrast to commercial polyolefin separators, most reported high heat-resistant separators synthesized by electrospinning, phase inversion and vacuum filtration still exhibited lower mechanical strength and could not withstand the large tension developed by the winding operation used during the battery assembly. Although the introduction of the materials with high strength such as inorganic nanoparticles can improve the strength of membranes properly, the ceramic content limits further improvement in mechanical strength. What's worse, the large pore sizes tend to become free path for the diffusion of cathode particles to anodes, and might cause local short-circuit. These problems still need to be addressed for the further commercial applications of those separators.

3.2 Lithium dendrite-proof separators

Lithium is generally regarded as a promising anode material due to the high reversible capacity (3,860 mAh g^{-1}) and low electrochemical redox potential (−3.040 V *vs*. SHE) [101]. However, the high reactivity of lithium metals and the serious dendrite problems seriously restrict the development of lithium-metal batteries (LMBs). Due to the high reactivity of lithium anodes, lithium metals will spontaneously react with electrolytes to form an uneven and fragile SEI layer [102]. The insulating SEI layer can temporarily prevent the further reaction between lithium metals and electrolytes. Unfortunately, the fragile SEI layer could not adapt to infinite volumetric change of lithium cathodes during the cycle and finally broke. The formed cracks would become nucleation points of lithium dendrites. Then, the generated lithium dendrites will provide preferred deposition sites for lithium and react with the electrolyte to form a new SEI layer, leading to excessive consumption of lithium and electrolytes and reducing the Coulombic efficiency of the battery. In addition, fractured lithium dendrites may form so-called dead lithium, which leads to increased polarization of the battery [21]. More seriously, the lithium dendrites may penetrate the separators, resulting in internal short-circuit and safety hazards. Therefore, researchers have adopted various methods for separators to inhibit the generation of lithium dendrites, including regulating the uniform lithium-ion transmission, constructing artificial SEI layers and eliminating lithium dendrites by the reaction. The cycle time of Li symmetric cells with representative lithium dendrite-proof separators is summarized in Table 3.

3.2.1 Regulating uniform lithium-ion transmission

Uneven pores in the separators will lead to the uneven transmission of lithium ions during the repeated lithiation/delithiation processes, which will lead to the uneven deposition of lithium and the formation of lithium dendrites. Faster diffusion and more uniform lithium flux of lithium ions by adjusting various factors will contribute to the uniform deposition of lithium ions and thus inhibit the growth of lithium dendrites [103,104]. One of the methods to regulate the uniform transmission of lithium ions is to regulate the structure of the separators, so as to form uniform pore size and pore distribution [53,55,105–107]. Pan *et al.* [55] prepared a tri-layer membrane of cellulose nanofibers (CNFs)/PE/CNFs. As the CNFs layer has a narrow pore diameter distribution, the composite membrane can provide a more uniform lithium-ion flux and form a uniform current distribution on the electrode. The evenly distributed current-

Table 3 Summaries of Li/Li symmetric cells with different separators

Separator	Coin type	Current density (mA cm^{-2})	Cycle time (h)	Ref.
CNFs/PE/CNFs	Li/Li	0.65	above 400	[55]
Li–MMT/PVDF–HFP	Li/Li	0.5 1	about 350 above 200	[105]
PDA/POSS–PE	Li/Li	2	about 200	[110]
PP@PLLZ	Li/Li	1	above 1000	[112]
NH_2–MIL-125(Ti)–PP	Li/Li	1	1250	[115]
BN–PE	Li/Cu	1	above 200	[121]
SrF_2–PP	Li/Li Li/Cu	0.25 0.25	350 1600	[122]
$PbZr_{0.52}Ti_{0.48}O_3$–PP	Li/Li	2	above 200	[123]
Garlics–PVDF/HFP	Li/Li	–	above 2000	[124]
PP/$MnCO_3$	Li/Li	1 2 3	above 2000 above 2000 above 2000	[125]
Si–PP–Si	Li/Li	0.5	above 2000	[130]
PEO/ANF	Li/Li	0.25	above 2500	[131]
Agarose	Li/Li	1	above 650	[133]
HAPs/PVA	Li/Li	0.5	above 600	[135]

density leads to more uniform lithiation/delithiation, forming a dense lithium deposition layer, reducing the risk of lithium dendrites piercing the separator, which will improve the stability of lithium anodes and the safety of LMBs (Figure 4 (a)). Zhao *et al*. [105] embedded a PVDF-HFP membrane into a layered montmorillonite membrane with an interatomic layered lithium channel by electrophoretic deposition. The separator with an interlaminar spacing of 1.31 nm could provide abundant active sites for Li^+ after absorbing electrolytes, which promoted the rapid transmission of lithium ions. In addition, the parallel intermediate layer unified the flow direction of lithium ions, thus promoting the uniform transmission of lithium ions and the uniform deposition of lithium on the negative electrode, effectively reducing the generation of lithium dendrites, and extending the cycle-life of LMBs.

Traditional polyolefin separators (such as PE and PP) have poor wettability. Hence the electrolyte is difficult to fill the pores of the membrane and cannot provide sufficient channels for the transmission of lithium ions, which is not conducive to the uniform transport of lithium ions and may lead to the generation of lithium dendrites, seriously threatening the safety of batteries (Figure 4(b)) [13,108,109]. Therefore, improving the wettability of the membrane can increase the transmission channel of lithium ions, thus making the transmission of lithium ions more uniform, which is beneficial to reduce the generation of lithium dendrites. The most common way to improve the wettability of the separators is to modify the polyolefin separators by introducing a coating layer of polymers (PDA, polyethylene oxide (PEO) and PMMA, *etc*.), inorganic ceramics (Al_2O_3, SiO_2, *etc*.), or composite materials on the polyolefin separators [32,110,111]. Ryou *et al*. [109] introduced a PDA coating on the surface of PE to improve the wettability of separators. Due to the introduction of hydrophilic PDA, the membrane electrolyte absorption rate and the ionic conductivity were improved. In addition, the enhanced wettability helps regulate the uniform transmission of lithium ions during the cycling process, thus inhibiting the formation of lithium dendrites. Therefore, batteries assembled by PDA-coated membranes showed a longer cycle-life and a better rate performance. In addition, Wang *et al*. [110] introduced an ultrathin PDA/POSS coating to the PE membrane surface in order to improve the battery performance. The ultrathin inorganic/organic composite coating improved the electrolyte wettability of separators, and significantly increased the ionic conductivity of the PE membrane (from 0.36 to 0.45 mS cm^{-1}), thus effectively suppressing the lithium dendrite growth and improving the cycle stability of the battery. In addition to surface modification of the polyolefin membrane, the use of polymers with excellent electrolyte affinity such as PVDF, PAN and PMMA as the membrane substrate is also an effective means to improve the wettability of the separators and regulate the uniform transmission of lithium ions.

During the transmission of lithium ions, the free anions moving in the opposite direction will also hinder the migration of Li^+, resulting in uneven lithium-ion transmission [112]. Therefore, functional materials that can immobilize the anions in the electrolyte are introduced to the separators, so that Li^+ can pass through the separator uniformly and transport to the electrode surface without being interfered by

anions, thus effectively promoting the uniformity of lithium deposition and reducing the formation of lithium dendrites [96,112–115]. Huo *et al*. [112] coated a layered porous composite solid electrolyte (CSE) composed of PVDF and $Li_{6.4}La_3Zr_{1.4}Ta_{0.6}O_{12}$ (LLZTO) on the one side of a PP separator to produce a composite separator with anti-lithium dendritic properties (Figure 4(c)). Among them, multiple three-dimensional (3D) fast lithium-ion channels in the composite separator could effectively redistribute uneven Li^+ flux and guide uniform deposition to form a uniform and dense Li deposition layer, reducing the risk of short-circuit. In addition, the CSE layer could fix free anions released from the lithium salt, thereby further regulating the lithium-ion concentration gradient and adjusting the uniform transmission of lithium ions, and inhibiting the formation of lithium dendrites. Among various materials, the metal-organic frameworks (MOFs) possessing open metal sites can spontaneously adsorb anions, thereby inhibiting the migration of anions, increasing the migration number of lithium-ions and promoting their uniform transmission [96,115–119].

Cui *et al*. [120] proposed that uneven heat distribution was one of the important factors that led to uneven distribution of lithium-ion flux and current density. The existence of temperature gradients inside the battery would cause uneven current distribution inside the battery, and local excessive current density often led to accelerated growth of lithium dendrites, making the battery more prone to short circuits. Luo *et al*. [121] used boron nitride (BN) nanosheets with well thermal conductivity as a simple coating for commercial separators to improve the cycle stability of Li metal anodes. The BN nanosheets could improve the heat distribution of the battery, and the lithium-ions flux was more uniform, then reducing the generation of lithium dendrites and improving the cycle stability of the battery. Therefore, adding high thermal-conductivity materials to improve the thermal-conductivity of the separators, which reduces the temperature difference within the battery, may be an effective way to adjust uniform lithium-ion transmission.

3.2.2 *Constructing artificial SEI layers*

On account of the excessive volume change of the lithium negative electrode during charging and discharging, the fragile SEI layer cannot adapt to this excessive change and breaks. The rupture of the SEI layer will expose the fresh Li to the electrolyte, forming a new SEI layer. The continuous rupture and formation of the SEI layer will continue to consume electrolytes and active lithium, and ultimately lead to high polarization, low charge and discharge efficiency of the battery, which will shorten the cycle-life of the battery and bring possible safety hazards. The formation of an artificial SEI layer on the lithium anode by introducing functional materials on the separator is considered to be a method

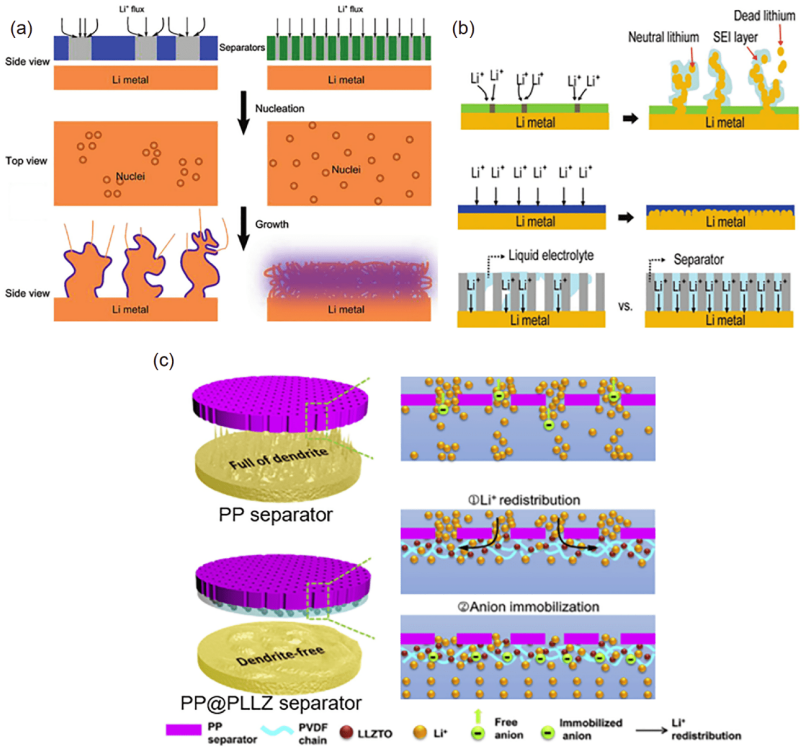

Figure 4 (a) The effect of uniform pore distribution on the morphology of the Li deposit. (b) The effect of the wettability of the separator on the uniform Li-ion flux. (c) Schematic illustrations of the Li deposition behaviours through PP separators and anion-immobilized PP@PLLZ separators. (a) Reprinted with permission from Ref. [55], Copyright 2018, John Wiley & Sons, Inc. (b) Reprinted with permission from Ref. [109], Copyright 2012, John Wiley & Sons, Inc. (c) Reprinted with permission from Ref. [112], Copyright 2020, Elsevier (color online).

that can effectively reduce the generation of lithium dendrites [122–126]. The strategy can stabilize the SEI layer and make the Li^+ flux on the electrode interface more uniform, thereby inhibiting the formation of lithium dendrites.

Li *et al*. [122] introduced strontium fluoride (SrF_2) microspheres to PP separators to stabilize the SEI layer and prevent the growth of lithium dendrites. The SrF_2 microsphere layer directly participated in the growth kinetics of the SEI layer and combined with the SEI layer to form a tough *in-situ* composite layer, making the SEI layer more stable. Moreover, lithium ions preferred to be adsorbed on the surface of SrF_2 microspheres, which generated a more uniform ion flux and reduced the risk of the formation of lithium dendrites (Figure 5(a)). Hu *et al*. [123] coated a PP separator with a $PbZr_{0.52}Ti_{0.48}O_3$ (PZT) layer (Figure 5(b)). The introduction of the PZT layer was reduced by the lithium-metal anode and formed a lead metal composite layer which adhered to the surface of the lithium anode and formed a more uniform Li^+ flux on the electrode interface, improving the lithium oxidation/deposition efficiency, thereby inhibiting the generation of lithium dendrites (Figure 5(c)).

Boateng *et al*. [124] designed a separator made of PVDF–HFP doped with garlic ingredients which exhibited strong binding energy with the inorganic salt in SEI. The organic sulfur in garlic improved the elasticity of the SEI to adapt to the volume change of the Li negative electrode during cycling, and inhibited the continuous consumption of lithium metal and made the lithium deposition more uniform, thus reducing the production of lithium dendrites and dead lithium (Figure 5(d)). The skeleton of the composite separator could also promote the uniform transmission of lithium ions by fixing anions and improve the stability of the lithium negative electrode. The $LiFePO_4$/Li half-cell using the separator showed almost no capacity decay after more than 3,000 cycles.

Yan *et al*. [125] reported an anti-dendritic strategy of coating manganese carbonate ($MnCO_3$) on one side of a PP separator. When $MnCO_3$ directly contacted the Li metal anode, the reaction of Li metal, $MnCO_3$ and the liquid electrolyte created a more stable SEI layer which prevented lithium dendrites from piercing the SEI layer during cycling, reducing the generation of lithium dendrites and the consumption of electrolytes, and enhancing the stability of the electrode. In addition, $MnCO_3$ was reduced by lithium and Mn nanoparticles (NPs) were generated on the surface of the Li electrode, thereby reducing the overpotential for nucleation and leading to large-size spherical Li deposition. This large-size lithium deposit had a small surface area, which was beneficial to inhibiting the formation of lithium dendrites and reducing the reaction at the lithium metal anode/electrolyte interface.

3.2.3 *Eliminating lithium dendrites through reaction*

Another strategy to eliminate lithium dendrites is the chemical reaction between lithium dendrites and the functionalized materials in separators [43,127]. Because active lithium will also be consumed and lead to a decrease in energy output, the separator that is made by this method may have a low energy density. With this in mind, separators designed with a layer-by-layer structure can help alleviate this problem [22].

Ye *et al*. [128] elaborately designed a PP/GO/PP tri-layer

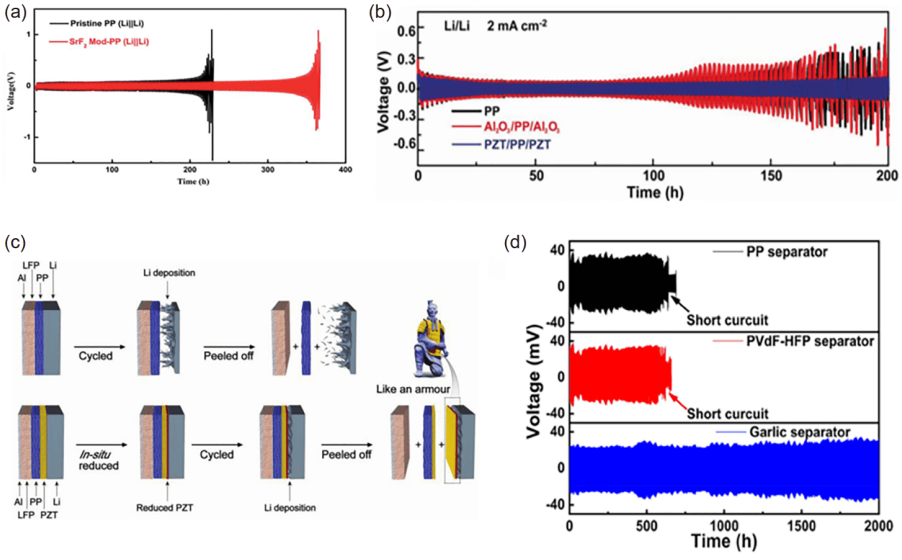

Figure 5 (a) Cycling properties of Li/Li cells separated by SrF_2-modified PP, tested at a current density of 0.25 mA cm^{-2}. (b) Schematic illustration of the PZT layer transferring to Li metal. (c) Cycling behaviours of Li/Li symmetric cells at 2 mA cm^{-2}. (d) Cycling behaviours of Li/Li symmetric cells separated by PP, PVDF–HFP, and a garlic separator. (a) Reprinted with permission from Ref. [122], Copyright 2019, the Royal Society of Chemistry. (b, c) Reprinted with permission from Ref. [123], Copyright 2020, John Wiley & Sons, Inc. (d) Reprinted with permission from Ref. [124], Copyright 2020, American Chemical Society (color online).

separator that can eliminate lithium dendrites. During the cycle, when lithium dendrites penetrate the PP membrane and contact with GO, GO would have a spontaneous oxidation-reduction reaction with lithium dendrites, thus preventing lithium dendrites from penetrating the whole separator, greatly extending the life of LMBs as well as improving the safety of the battery. In addition, thanks to the structure of the tri-layer separator, the GO will not directly contact the Li foil, so it would not cause redox reactions before Li dendrites penetrate the separator, avoiding unnecessary consumption of metallic Li. In addition, Liu *et al*. [129] also designed a similar PP/SiO_2/PP trilayer separator. Silica nanoparticles reacted with Li dendrites through a solid-state conversion reaction to effectively etch away lithium dendrites and slow down their further growth, and the method effectively delayed the time for lithium dendrites to pierce the polyolefin separator and extended the battery life.

Although the tri-layer separator can effectively avoid the direct contact between functional materials and metallic lithium, the thickness of the three-layer separator is too large to be suitable for thin and light batteries, and it is not conducive to improving the energy density of the battery. For this reason, Chen *et al*. [130] introduced a thin silicon coating (about 2 μm) on the PP separator to eliminate lithium dendrites to avoid lithium dendrites from piercing the separator and causing short circuits, which greatly improved the stability and cycle life of lithium metal anodes. The cycle life of the lithium symmetrical battery using the separator was more than 1,000 h (current density is 0.5 mA cm^{-2}). In addition, silicon and lithium metal form a silicide-rich SEI, which not only could prevent lithium loss caused by the contact of lithium with the electrolyte and the silicon coating, but also could supplement the lithium loss during the cycle. Zhang *et al*. [42] coated a "lithium-killing" layer composed of TiO_2 nanoparticles embedded in a porous Kynar polymer matrix on one side of the PP separator. When assembling the battery, the composite layer containing TiO_2 was placed to face the positive electrode, avoiding direct contact between the TiO_2 and the lithium negative electrode. The TiO_2 could react with the lithium dendrites penetrating the polyolefin membrane to prevent the short circuit problem caused by the lithium dendrites.

The strategy of eliminating lithium dendrites by reactions is only applicable to the situation where only a small amount of lithium dendrites are generated. When many lithium dendrites are generated, the functionalized materials on the separator will not be able to completely remove the lithium dendrites in time. As a result, lithium dendrites eventually pierce the separator and cause a short circuit. In addition, the formation and reaction of many lithium dendrites will inevitably lead to the consumption of active lithium, which will eventually lead to a decrease in capacity. Therefore, other ways such as adjusting the transmission of lithium ions should also be used to reduce the formation of lithium dendrites as a supplement.

3.3 Separators with high mechanical stability

Mechanical strength is an important factor in assessing whether the separator is sufficiently safe or not. During the battery assembly process, the separator must be strong enough to withstand the stress generated by the battery during the winding manufacturing process. However, the emphasis on more specific power in the mobile devices has led to the design with light-weight and thinner layers of separators. They are vulnerable to mechanical abuses such as crushing, bending and dropping. The mechanical deformation of the separators might lead to the final failure of LIBs. In addition, the separator should have sufficient puncture strength to cope with the puncture of the lithium dendrites generated during the battery cycle, to prevent the lithium dendrites from penetrating the separator and ultimately leading to the short circuit of the battery. In this chapter, we will introduce the development direction of designing separators with high mechanical stability which could tolerate external mechanical impact or internal lithium dendrite piercing, including Li-dendrite resistant separators, electrospun nonwoven mats with high mechanical strength, separators with high tensile strength, stretchable separators.

3.3.1 Li-dendrite resistant separators

The currently used commercial separators do not have sufficient mechanical strength to resist the penetration of lithium dendrites, and are easily penetrated by lithium dendrites during cycling, which would cause a short circuit and pose a greater safety risk. Therefore, the development of a separator with ultrahigh mechanical strength can effectively delay the time for dendrites to pierce the separator and extend the life of LMBs (Figure 6(a)). The prediction is that separators with high shear modulus (G′>7 GPa, which is 1.8 times higher than that of metallic lithium) can prevent dendrite proliferation [23].

Polymer fibers with ultra-high shear modulus, such as Kevlar fiber, PEEK and PBI, have been used to prepare lithium-resistant dendrites [70,131,132]. Tung *et al*. [131] used a layer-by-layer self-assembly method to combine aramid nanofibers (ANFs) and solid ion-conducting PEO to prepare dense and uniform PEO/ANFs separators. The film had ultrahigh mechanical strength (tensile strength ~170 MPa, Young's modulus ~5 GPa and shear modulus ~1.8 GPa), which effectively inhibited the growth of copper dendrites (the Young's modulus of copper is 26 times higher than that of lithium. Hence, if the local mechanical properties of the separator were sufficient to prevent the harm caused by copper dendrites, it would also inhibit the growth of li-

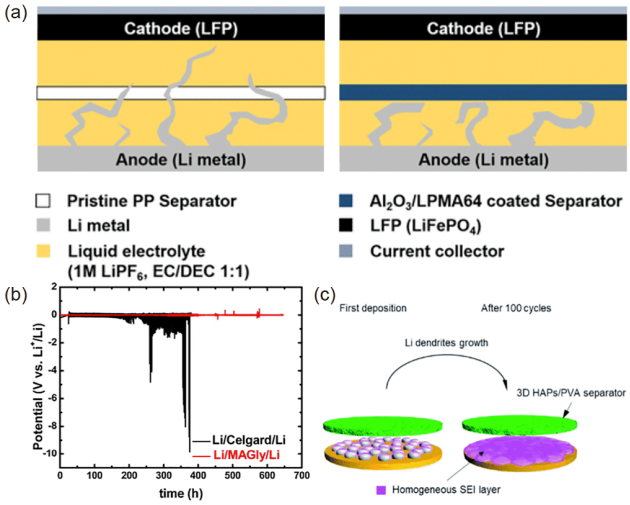

Figure 6 (a) Schematic depiction of the mechanical suppression preventing lithium dendrite formation. (b) Voltage profiles of the symmetric cells Li/Li with MAGly or Celgard as a separator a current density of 1 mA cm^{-2}. (c) Schematic illustration showing the growth process of dendritic Li on the surface of the copper substrate with the 3D HAPs/PVA separator. (a) Reprinted with permission from Ref. [134] Copyright 2016, American Chemical Society. (b) Reprinted with permission from Ref. [133], Copyright 2020, Elsevier. (c) Reprinted with permission from Ref. [135], Copyright 2019, The Royal Society of Chemistry (color online).

thium dendrites) and extended the cycle-life of the battery. In addition, it was found that the (PEO/ANF) separator could suppress the growth of dendrites by applying pressure to the electrodeposition area, thereby obtaining a uniform and dense deposition layer. Blin *et al*. [133] used agarose as a biopolymer and glycerol as a plasticizer to prepare a polymer separator with high elasticity and stiffness. Due to the high rigidity of the composite film (~1 GPa at 15 °C), it could effectively prevent dendrite growth and greatly extend the cycle-life of the battery (at a current density of 1 mA cm^{-2}, a lithium symmetric battery using an agarose separator can work stably for more than 700 h (Figure 6(b)).

The introduction of high modulus inorganic ceramic coatings into conventional polyolefin separators can also significantly improve the mechanical strength and thermal stability of the separators. Na *et al*. [134] designed a kind of UV light-cured Al_2O_3 ceramic coated polypropylene separator with poly(phenyl-*co*-methacryloxypropyl)silsesquioxane (LPMA64) as the adhesive. The prepared separator had an ultra-high elastic modulus (7.3 GPa), which was greater than that of metallic lithium (4 GPa), and the elastic modulus required to inhibit the growth of lithium dendrites (6.2 GPa), thus effectively inhibiting the growth of lithium dendrites as well as improves the cycle stability of the battery at high C-rates. Besides, inorganic-organic composite materials were often used in the preparation of dendritic resistant membranes with high mechanical strength [135–137]. Wang *et al*. [135] prepared an organic-inorganic composite membrane composed of degradable polyvinyl alcohol (PVA) and hydroxyapatite nanorods (HAPs) by freeze-drying. The Young's modulus of the composite separator was 40 GPa higher than that of the polyolefin separator (a solid layer with a Young's modulus greater than 6 GPa can fully retard the growth of Li dendrites), and hence it could effectively inhibit the growth of lithium dendrites (Figure 6(c)).

Liang *et al*. [19] proposed through mechanical stress calculation and analysis that the curved shield surface has the effect of reducing the stress in the face of lithium dendritic puncture, and when the curvature of the shield is equal to the curvature of the dendrite tip, the stress reduction is the most obvious. Based on this theory, researchers spin-coated modified nanoparticles on the polyolefin separator, and made the curvature equal to the tip of the lithium dendrite, thereby effectively reducing the stress, inhibiting the puncture of the lithium dendrites to the separator, and avoiding short circuits in LMBs. The test found that the Li/Li symmetric battery using this nanoshield-modified separator could maintain long-term stable lithium deposition for more than 110 h, and its life was five times as much as that of symmetric batteries with polyolefin separators.

3.3.2 *Nonwoven separators with high mechanical strength*

As mentioned above, electrospun non-woven mats as separators were favored by researchers due to their high porosity, 3D network structure and high specific surface area. However, the electrospun fibers were in a disorderly stacked state and lacked effective bonding points, which led to poor mechanical strength and made them difficult to resist the stress generated in the battery assembly process and puncture of lithium dendrites during cycling, which was not conducive to the safe operation of the battery, limiting the large-scale applications of electrospun separators [138]. To this end, researchers adopted a variety of methods to enhance the mechanical strength of electrospun membranes.

One of the most effective methods is to prepare fibers with a core-shell structure by coaxial spinning. For example, Sun *et al*. [74] designed a kind of lithium-ion battery separator with PI nanofibers as a core material and PBI as a reinforced sheath material (PBI@PI). This kind of lithium-ion battery separator exhibited ultra-high strength (59 MPa) through self-bonding and self-compression technology (Figure 7(a)). Zhao *et al*. [69] created a core-shell PI@fluorinated poly(*m*-phthalamide) (F-PMIA) nanofiber separator by coaxial electrospinning, which coupled hardness with softness (Figure 7(b)). The PI core with fracture toughness served as a stable and powerful skeleton support, which ensured the structural stability of the PI@F-PMIA separator. The separator with this structure had a relatively high mechanical strength of 15.2 MPa. In addition to preparing fibers with a core-shell structure by coaxial spinning, inorganic ceramic particle layers such as TiO_2 and SiO_2 could be chosen to grow on the electrostatic fiber to obtain non-woven com-

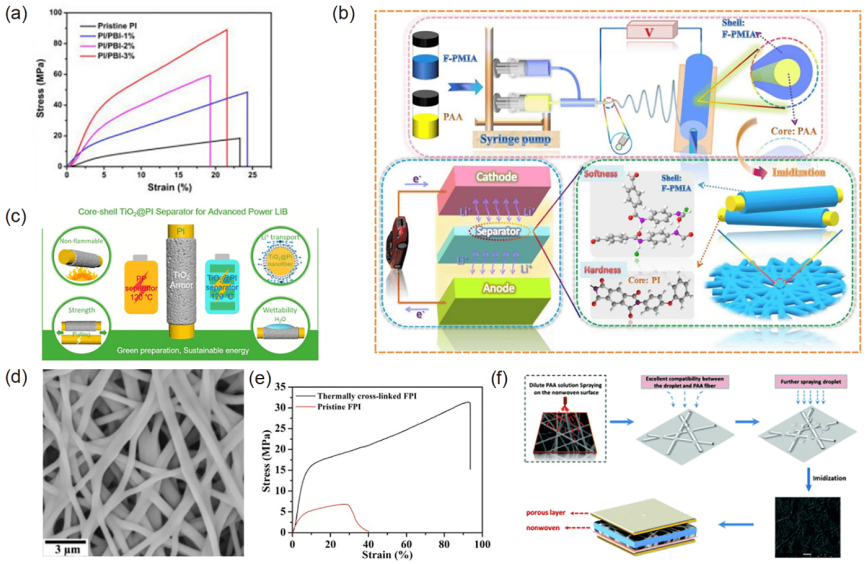

Figure 7 (a) Tensile stress-strain curves of the pristine PI, PI/PBI-1%, PI/PBI-2%, and PI/PBI-3% membranes. (b) The schematic illustration of the preparation of the functionalized PI@F-PMIA separator and the resulting battery assembling process. (c) Schematic of the structure for the *in-situ* SiO_2@(PI/SiO_2) hybrid separator. (d) SEM images of thermally cross-linked FPI nanofibers membranes. (d) Stress-strain curves of pristine and thermally cross-linked FPI nanofiber membranes. (f) Mechanism of the formation of the porous-layer-coated PI nanofiber membranes through *in-situ* self-bonding and micro-crosslinking technique (a) Reprinted with permission from Ref. [74], Copyright 2019 Elsevier. (b) Reprinted with permission from Ref. [69], Copyright 2021, Elsevier. (c) Reprinted with permission from Ref. [17], Copyright 2019, American Chemical Society. (d, e) Reprinted with permission from Ref. [78], Copyright 2018, Elsevier. (f) Reprinted with permission from Ref. [141], Copyright 2018, The Royal Society of Chemistry (color online).

posite separators to enhance their mechanical strength [17,139,140]. For example, Dong *et al.* [17] grew a layer of TiO_2 nanoparticle shells *in situ* on PI fibers (Figure 7(c)). Thanks to this layer of *in-situ* armoring, the *in-situ* TiO_2@PI composite membrane showed good thermal stability at 300 °C and excellent mechanical strength (27.6 MPa), which was better than that of pristine PI separators (5 MPa).

The artificial introduction of cross-linking points between the fibers is another effective strategy to enhance the mechanical strength of the electrospun separators. Kong *et al.* [78] placed a fluorinated polyimide non-woven fabric film at 300 °C for 15 s for a simple thermal cross-linking treatment. The thermally cross-linked FPI fibers adhere each other to form many effective bonding points, which greatly enhances the tensile strength of the non-woven film (31.7 MPa, which is 5 times as much as that of the original FPI film) (Figure 7 (d, e)). In addition, the thermally cross-linked separator had a more uniform pore size distribution, which was conducive to the uniform transmission of lithium ions and reduced the generation of lithium dendrites. Sun *et al.* [141] obtained a PI non-woven fabric film by spraying dilute PAA solution on both sides of PAA non-woven fabric and performing heat treatments in sections. Since PAA was partially dissolved in the dilute PAA solution, the resulting PI non-woven mat separator formed many welded junctions, forming a mutually cross-linked grid structure (Figure 7(f)). The self-adhesive and micro-cross-linked structure formed *in-situ* effectively enhanced the mechanical strength of the PI film, and the tensile strength increased from 5 to 28 MPa.

3.3.3 *Separators with high tensile strength*

The mechanical properties of the separator are characterized by tensile strength and puncture strength. Owing to sufficient strength to resist the puncture of lithium dendrites, the separator should also have sufficient tensile strength to cope with the stress caused by the winding of the separator as well as the battery assembling, and the impact hurt caused by battery drop and collision. The weak tensile strength will make the battery unable to withstand the stress of battery assembly and rupture, and eventually lead to short circuit and threaten the safe operation of the battery. In addition, the separator should also have a high Young's modulus, which helps maintain structural integrity and prevent rupture in the event of an accidental collision.

Using high tensile strength materials as the base film of the separator is a good way to sustain the tensile strength of the separator. Patel *et al.* [142] obtained ANF membranes with ultra-high modulus through vacuum filtration. The Young's modulus of the ANF separator at breakage was 8.8±1.1 GPa, which was ~1,000% higher than that of commercial polyolefin separators, and the tensile strength was as high as 253±18 MPa (Figure 8(a)). The ANF separator could withstand high loads or external forces without deformation or failure, which greatly improved the safety of the battery. In addition, Liu *et al.* [143] prepared polyoxymethylene (POM)/cellulose nanofiber blend separators by non-solvent induced phase separation (NIPS). Thanks to the high crystallinity and high mechanical strength of POM and CNF, the separator exhibited excellent tensile strength (116 MPa) and

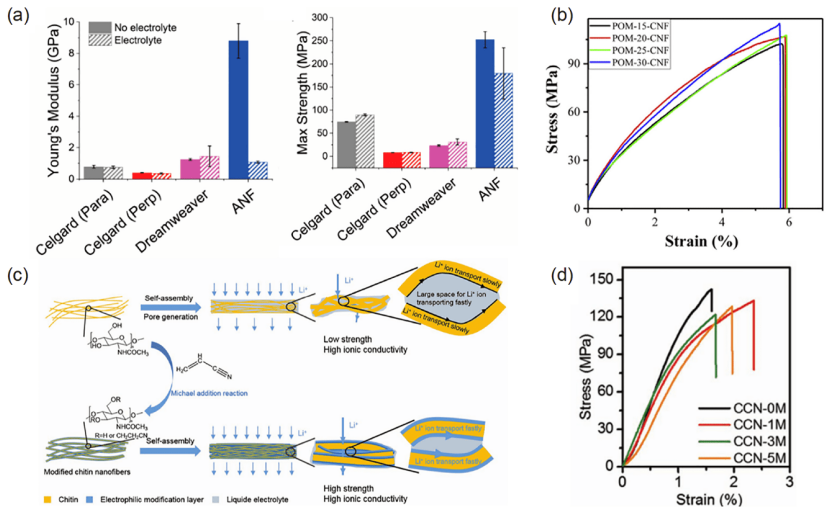

Figure 8 (a) Young's modulus and maximum strength for different separators when they are dry (solid bars, no electrolyte) and wet (dashed bars, in electrolytes). (b) Stress-strain curves of POM-CNF blend separators. (c) Schematic diagram of multi-void chitin plasma membrane with pore forming agent added and dense cyanoethyl chitin nanofiber (CCN) membrane. (d) Stress−strain curves of the CCN separators. (a) Reprinted with permission from Ref. [142], Copyright 2020, American Chemical Society. (b) Reprinted with permission from Ref. [143], Copyright 2018, Elsevier. (c, d) Reprinted with permission from Ref. [90], Copyright 2019, John Wiley & Sons, Inc. (color online).

Young's modulus (6.07 GPa) (Figure 8(b)).

In a general way, the porosity of the separator is inversely related to mechanical strength. A high porosity will reduce the mechanical strength of the separator, which is not conducive to the safety of the battery. However, the low porosity is not conducive to the transmission of lithium ions and affects the performance of the battery. In order to coordinate the relationship between mechanical strength and ion transport, Zhang *et al*. [90] reported a dense chitin membrane with high mechanical strength. Due to the hydrogen bonding of the hydroxyl groups between the chitin nanofibers, the prepared membrane would be dense and non-porous, and therefore had very low ionic conductivity. In order to improve the ionic conductivity of the chitin membrane, it is usually necessary to add a pore former to increase the porosity of the chitin membrane which might weaken the mechanical strength of the membrane (Figure 8(c)). In order to solve this problem, the authors grafted cyanoethyl onto the surface of chitin to prepare a cyanoethyl chitin membrane with a dense structure. This dense membrane had a high mechanical strength (120 MPa), much higher than PP membrane (90 MPa) and porous chitin membrane (80 MPa) (Figure 8(d)). In addition, Li^+ can quickly migrate along the chitin nanofibers grafted with cyanoethyl, the obtained separator soaked with electrolytes had a relatively suitable ionic conductivity (0.45 mS cm^{-1}). This method also provided a new perspective for improving the mechanical strength of separators.

3.3.4 Stretchable separators

In recent years, with the development of electronic device technology, more and more electronic devices are developing to be thinner, wearable, and flexible. For example, Huawei and Samsung have successively introduced foldable mobile phones in recent years. However, the emergence of these flexible and wearable electronic devices has higher mechanical flexibility requirements for their power supplies, so how to make the battery bend is a technical problem that must be solved. In order to maintain stable battery performances, the separator must have reversible shape deformation and high stretchability.

Generally speaking, one of the strategies to realize stretchable membranes is to construct 2D/3D porous microstructures [144]. The 2D/3D porous microstructure strategy means that the porous network can withstand strain through deformation before the material in the 2D/3D network undergoes direct strain, so that it has good performance under tension. For example, Li *et al*. [145] prepared HAP NWs/CFs separators with high flexibility (Figure 9(a)), benefiting from the formation of a layered cross-linked network structure between hydroxyapatite nanowires and cellulose fibers through hybridization, giving the separator high flexibility and mechanical strength, so that the separator underwent repeated bending and twisting, and there was no visible mechanical damage after folding (Figure 9(b)). Shin *et al*. [146] prepared a stretchable poly(styrene-*b*-butadiene-*b*-styrene) (SBS) separator through the NIPS method. Due to the inherent elastic properties of thermoplastic elastomer (TPE) and a well-developed cavity structure of the SBS separator, this membrane has extremely high stretchability. Under 100% strain, 200% uniaxial stretching and 60% biaxial stretching were effectively realized without any damage, and good tensile strength was maintained in 100 stretch/release experiments (Figure 9(c)).

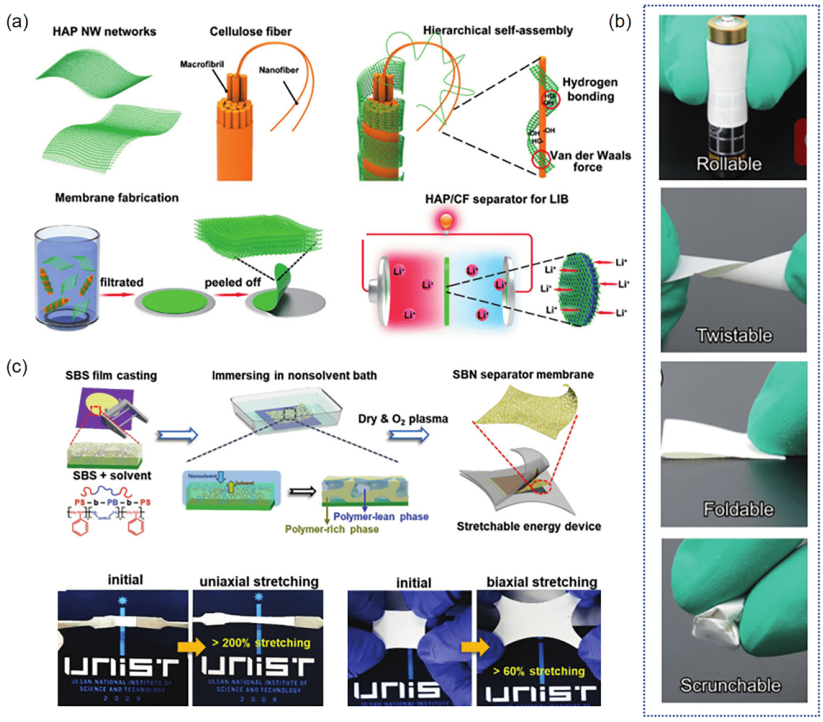

Figure 9 Schematic diagram of HAP/CF separator structure and preparation process. (b) High flexibility of the HAP/CF separator under different bending conditions. (c) Fabrication process of the SBN and digital photographs of the SBN separator membrane under uniaxial stretching and biaxial stretching. (a, b) Reprinted with permission from Ref. [145], Copyright 2017, John Wiley & Sons, Inc. (c) Reprinted with permission from Ref. [146], Copyright 2018, John Wiley & Sons, Inc. (color online).

In the process of repeated bending of the battery, the gap between the positive and negative electrodes is constantly changing with the degree of bending, which will cause the internal resistance of the battery to continue to rise and affect the cycle stability of the battery. Therefore, flexible batteries must have better cathode-separator-negative interface stability. Liu *et al*. [147] prepared an elastic-sticky PU/PVDF separator with high stretchability through the electrospinning method. This kind of separator could be firmly adhered to the electrode after rolling at 60 °C. The delamination of the electrode and the separator was prevented, and the stability of the interface between the electrode and the separator was enhanced. In addition, the separator also had high tensile strength and could provide 120% strain, which was beneficial to avoid it from breakage and detachment in the wave-shaped battery.

3.4 Novel multi-functional separators

Ideally, a high-safety separator should have several universal properties, including: (i) high thermal stability, which can ensure battery safety under high-temperature operation. (ii) High ion conductivity, which can adjust uniform lithium-ion channels and slow down the growth of lithium dendrites. (iii) Robust mechanical strength and high flexibility, which can prevent the membrane from rupturing during battery assembly and cycling. Nevertheless, these characteristics are not enough to meet all the requirements for high-safety separators in different working environments. Therefore, in order to develop a next-generation LIB with higher safety and superior performances, it is necessary to develop new types of separators with more functions.

3.4.1 Flame-retardant separators

It has been generally recognized that the safety of LIBs is closely associated with the highly flammable liquid organic electrolytes such as ethylene carbonate (EC) and diethyl carbonate (DEC) [148]. If the thermal runaway happens, an increase of internal temperature will trigger flammable liquid electrolytes ignited, eventually leading to fire and explosion. An effective and direct way is to add flame retardant additives to the existing electrolytes or to use non-flammable electrolytes instead of flammable electrolytes [102,149–153]. These flame-retardant additives are usually based on phosphorus or halogen molecules, and exhibit flame retardancy through physical isolation mechanisms or chemical free-radical scavenging processes. However, this strategy often requires considerable flame retardants, which will increase the viscosity of the electrolyte and reduce the ionic conductivity as well as the capacity of batteries. Another proposed strategy to solve this problem involves incorporating the flame retardant such as triphenyl phosphate (TPP),

polyphenylene sulfide (PPS), PBI or inorganic non-flammable ceramic additives inside the protective polymer shell of microfibers, avoiding the flame retardant from directly contacting with the electrolyte, which would not deteriorate the electrochemical performance of LIBs [74,145,154–156].

Cui *et al*. [157] developed a novel "intelligent" non-woven separator with thermal trigger flame retardancy (Figure 10 (a)). The flame retardant TTP was encapsulated in a protective polymer shell (PVDF–HFP) to prevent the flame retardant from dissolving directly into the electrolyte. In addition, PBI possessed outstandingly inherent flame retardancy and good electrolyte wettability due to the existence of rigid structures and the polar nitrogen atoms of imidazole rings. As mentioned before, Sun *et al*. [74] prepared a novel core@sheath nano-fiber membrane with the PI nanofiber as the core material and PBI as the reinforced sheath material *via* the self-bonding and self-compression technique. The PI/PBI-2% membrane also displayed outstanding self-extinguishing ability when it was exposed to fire and showed better thermal stability than the pristine PI membrane due to the existence of the PBI sheath material. Recently, Zhao *et al*. [158] designed a heat-proof and fire-proof bifunctional separator by coating ammonium polyphosphate (APP) particles on a ceramic-coated separator modified with phenol-formaldehyde resin (CCS@PFR) (Figure 10(b–d)). APP served as a flame retardant by the physical isolation mechanism. When the temperatures were above 300 °C, APP decomposed, forming a dense polyphosphoric acid (PPA) layer, which acted as a barrier to isolate the combustibles from the highly reactive oxygen released from the cathode.

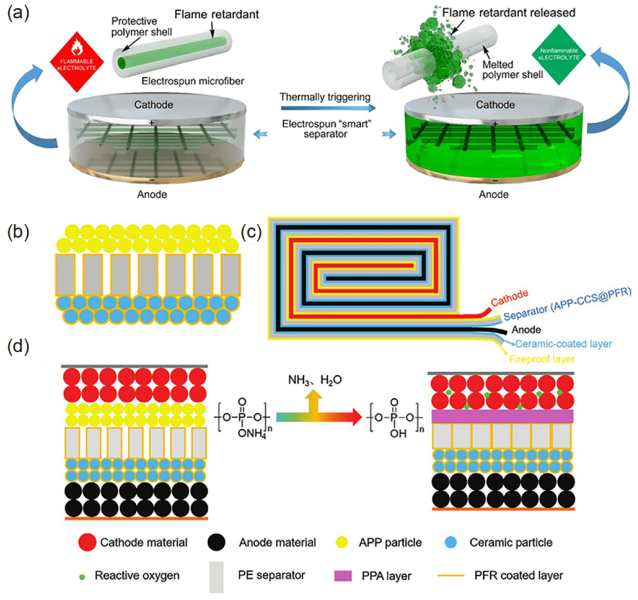

Figure 10 (a) Schematic of the "smart" electrospinning separator with thermal-triggered flame-retardant properties for LIBs. (b) Schematic of the APP-CCS@PFR. (c) Structure of high-safety LIBs assembled with APP-CCS@PFR; and (d) safety mechanism of APP-CCS@PFR for LIBs. (a) Reprinted with permission from Ref. [157], Copyright 2017, American Association for the Advancement of Science. (b–d) Reprinted with permission from Ref. [158], Copyright 2020, John Wiley & Sons, Inc. (color online).

Inorganic ceramic, one of the most eco-friendly and chemically inert refractory materials, has been incorporated with organic frameworks to function as separators. Kong *et al*. [140] reported a novel method by *in-situ* forming silica@-silica-imbedded PI (*in-situ* SiO_2@(PI/SiO_2)) nanofabric as a new high-performance inorganic-organic hybrid separator (Figure 11(a, b)). The PAA/TEOS nanofiber membrane underwent a thermal treatment, during which the PAA was converted into PI and TEOS migrated uniformly from inside to the surface of the nanofiber. After that, the PI/TEOS nanofabric was subjected to *in-situ* hydrolysis and formed the SiO_2 shell. Therefore, the hybrid separator showed good thermomechanical stability at 300 °C, and fire resistance. Jing *et al*. [159] reported a non-woven ZrO_2 ceramic membrane with flame-resistant performance *via* polymeric electrospinning followed by a high-temperature organic burn-off (Figure 11(c)). After firing the precursor membrane in air at 800 °C for 3 h, the membrane well maintained the appearance of the defect-free precursor membrane. The pure material ZrO_2 separator not only exhibited a remarkable flexibility, finely tailored porosity, but also showed much greater thermal stability and fire-resistance than the commercial Celgard separator (Figure 11(d)).

3.4.2 *Intelligent protective separators*

Although many thermal stability separators have been developed, their thermal shutdown performances are moderate and the inner electrochemical reactions under thermal runaway conditions still go on. These side-reactions subsequently accelerate the temperature increasing through a dangerous positive feedback mechanism, producing excessive heat and flammable gas within a very short time. Eventually, this extreme condition leads to fire or explosion of the cells. Currently, smart strategies to enable stimuli responsiveness and active protection against thermal runaway have been reported.

One of the targets to design smart separators is to avoid internal shorting. Employing multi-layer membranes with shutdown function as a separator is a promising and effective method. In general, a multi-layer separator with the shutdown property usually includes a fusible interlayer sandwiched with two robust outer layers. If temperature rises, the robust outer layers with high thermal stability can be strong enough to prevent shrinkage and avoid the short circuit of electrodes. Meanwhile, the fusible interlayer will melt to block the membrane pores, terminating the reactions by completely inhibiting the transfer of lithium ions. For example, commercial three-layer composite PP–PE–PP and PP–PE are commonly used as a thermal shutdown separator [160,161]. A 35 °C-buffer between PE shutdown and PP melting (165 °C) is obviously not enough to protect large

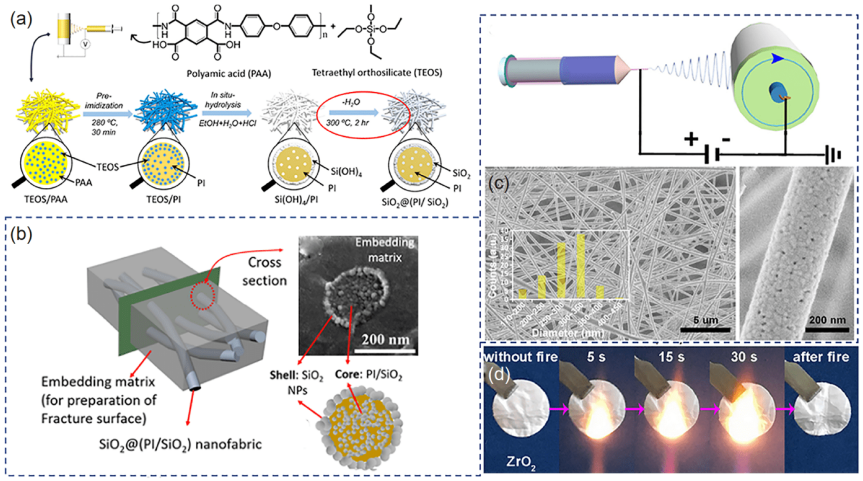

Figure 11 (a) Schematic of the fabrication strategy for the *in-situ* SiO_2@(PI/SiO_2) hybrid separator by combining electrospinning and inverse *in-situ* hydrolysis. (b) Illustration of preparation of the cross section of *in-situ* SiO_2@(PI/SiO_2) hybrid nanofibers for SEM imaging. (c) Schematic of the electrospinning device and low/high magnification SEM images. (d) Fire-resistant tests of the ZrO_2. (a, b) Reprinted with permission from Ref. [140], Copyright 2019, American Chemical Society. (c, d) Reprinted with permission from Ref. [159], Copyright 2020, Elsevier (color online).

LIBs from thermal runaway. Thermal inertia after PE shutdown can easily increase the temperature to the melting-point of PP, resulting in serious short circuit. The PP outer layers are not strong enough due to low melting-point and deformation temperature. The most common method is to use a polymer with a high melting-point, such as PBI, PI, polyetherimide (PEI) to enlarge the difference between the melting-point of the thermosensitive materials and the substrate, so that the composite separator can perform thermal shutdown behaviors, avoiding worse situation [162,163].

Replacing the PP outer layer of the commercial separator PP/PE/PP with high melting-point polymers can achieve safer battery systems. Li *et al.* [164] designed a sandwich-like composite membrane with a porous PBI layer introduced on both sides of a PE separator by a typical phase inversion method. This composite membrane exhibits super-high thermal stability. The PBI/PE/PBI (referred to PBIE) showed no dimensional shrinkage up to 200 °C and the prepared PBIE membrane could easily shut the battery down at about 140 °C (Figure 12(a–d)). Besides, Sun *et al.* [165] reported a new and practical tri-layer separator fabricated *via in-situ* welding technique, using PBI@PI nanofiber mats as the structural support and melt-processable PEI non-woven mats as the cross-linking interlayer (Figure 12(e)). The melting-point of the inner layer increased at approximately 235 °C. When the PEI interlayer started melting and the melting-point of PBI@PI was much higher (Figure 12(f, g)), ensuring that the battery stops working at high temperature. Li presented a tri-layer membrane featured with double amido-functionalized PEEK outer layers and a PMMA interlayer [166]. The fusible PMMA interlayer could melt to block the pores of separators when the temperature increased to higher than 100 °C and the out layer ensured high maximum operating temperature (350 °C). The wide shutdown temperature window (100–270 °C) of the separator improved the high temperature safety of the batteries.

Another target to design smart separators is to avoid overheating. This separator can ensure the ion channel cutting off at relative lower temperatures (often lower than the melting-point of the polyolefin separator) when overheating occurs. In other words, if the thermal shutdown can occur earlier, the dimensional stability of the separator can be kept for a longer time. Some high thermal sensitivity and low melting-point materials like EVA, or PE microspheres are good choices [14,167,168]. Jiang *et al.* [169] successfully prepared a poly-(lactic acid/poly-(butylene succinate) (PLA@PBS) core-shell separator with thermal shutdown by using a simple coaxial electrospinning process (Figure 13(a)). PLA was used as the core material because of its excellent thermal dimensional stability and mechanical strength, and PBS was used as the shell material because of its strong affinity to liquid electrolytes and suitable closing (melting) temperature (Figure 13(b)). The PLA@PBS membrane did not shrink after treating at 170 °C for 15 min, showing good dimensional stability (Figure 13(c)). Jiang *et al.* [95] prepared a temperature-dependent switching PVP@TiO_2 separator by the electrospinning method (Figure 13(d)). The PVP@TiO_2 separator could work at 180 °C. The battery could be reversibly closed at 60 °C through the reaction between PVP and electrolytes, and then revived like a new battery after being brought back to room temperature (Figure 13 (e, f)).

Developing a smart, self-protection separator in response to the inner risk is a promising strategy to expand the application of LIBs. However, except for the high cost, further improvements are needed to be made before the practical

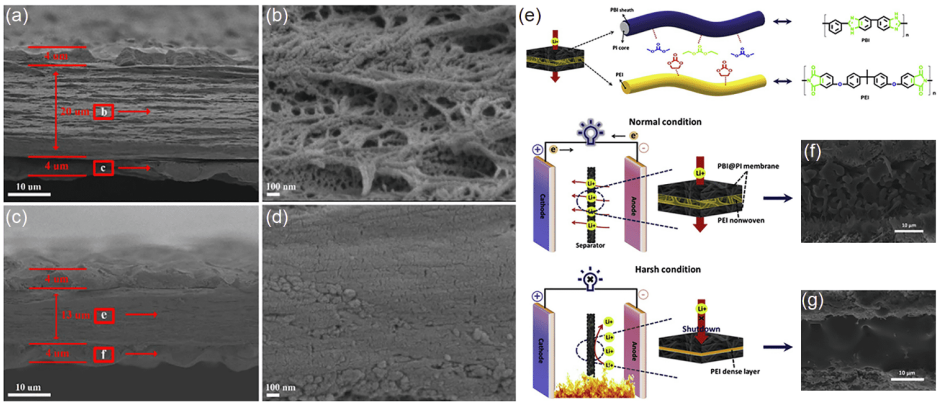

Figure 12 (a) The cross-section and (b) magnified cross-section images of boxes in (a) of a PBIE membrane before heat-treatment. (c) The cross-section and (d) magnified cross-section images of boxes in (c) of a PBIE membrane after heat treatment at 140 °C for 0.5 h. (e) Schematic principle of the inter-action between separator and the electrolyte. Illustrations of (f) the normal operation and (g) the shutdown function of PBIE separators in applications. (a–d) Reprinted with permission from Ref. [164], Copyright 2017, Elsevier. (e–g) Reprinted with permission from Ref. [165], Copyright 2020, Elsevier (color online).

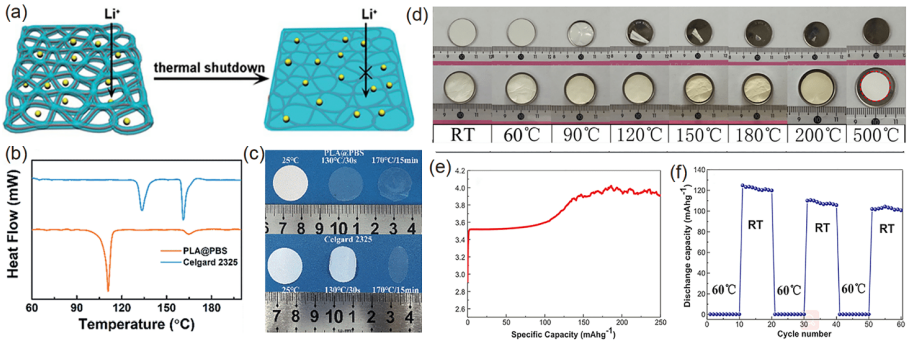

Figure 13 (a) Schematic representation of the coaxial fiber separator shut-down concept for LIBs. (b) DSC curves of the PLA@PBS and Celgard 2325 separator (c) Photographs of the PLA@PBS and Celgard 2325 separators before after treatment at 130 °C for 30 s and 170 °C for 15 min. (d) Thermal stability tests of PP and PVP/TNT separators. (e) Charge curve of the cell with PVP/TNT separators at 60 °C. (f) On/off function of the as prepared PVP/TNT separators. (a–c) Reprinted with permission from Ref. [169], Copyright 2017, Royal Society of Chemistry. (d–f) Reprinted with permission from Ref. [95], Copyright 2018, Elsevier (color online).

applications of these lab-scale smart devices.

3.4.3 *High thermal conductivity separators*

Electrochemical reactions in a LIB generate heat, which influences the temperature distribution. And the temperature distribution in turn governs the electrochemical reaction kinetics and ionic charge transport, and thus affects the performance of batteries. As described above, the uniform temperature distribution inside the battery can reduce the growth of lithium dendrites to a certain extent. Unfortunately, the commercial polyolefin separators exhibit low thermal conductivity (<1.0 W m^{-1} K^{-1}). The polyolefin separator modified with thermal conductivity materials might achieve uniform heat diffusion, which efficiently suppresses the Li dendrites and stabilizes the redox reactions.

Boron nitride (BN) is regarded as one of the most important thermally conductive materials, mainly owing to its high thermal conductivity (750 W m^{-1} K^{-1}), electrically insulating properties, as well as its outstanding mechanical strength (Young modulus of 80 GPa) [41,97,121,170,171]. The BN-coated separator with good thermal conductivity can provide a more homogenous temperature distribution to enable uniform nucleation. Liu *et al*. [172] designed a novel and safe separator by integrating thermally management BN nanosheets into PVDF-HFP *via* an advanced extrusion-based 3D printing technique (Figure 14a). When the local heat source was incident on the separator, the localized heat can be diffused effectively along the BN-separator, yielding a low central temperature. Compared with the commercial separator, the BN separator provided a more homogenous temperature distribution and showed a stable Coulombic efficiency of 92% after 90 cycles at 1 mA cm^{-2} in Li/Cu cells (the control cell decreased to 70% after 30 cycles). Luo and co-workers [121] also presented a thermally conductive separator coated with BN nanosheets with a high thermal conductivity of 82 W m^{-1} K^{-1}. From the detection of the temperature distribution on the infrared camera, it could be seen that the BN-coated separators enhanced heat spreading

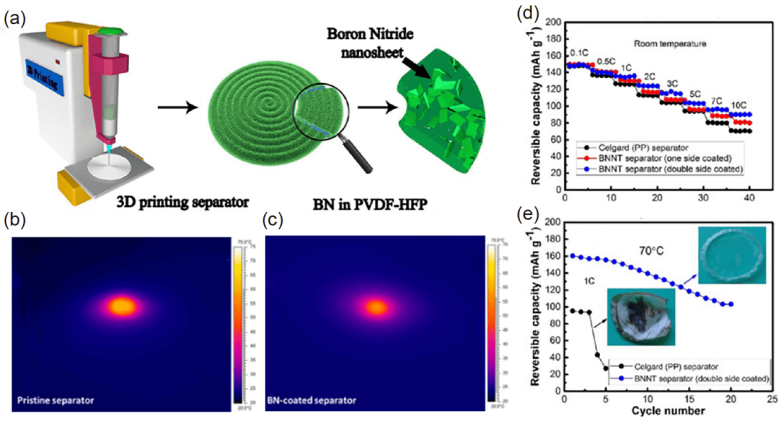

Figure 14 (a) Schematic illustration of the 3D printing apparatus, the BN in PVDF-HFP separators and the corresponding composition and structure. (b, c) Temperature distribution images. (d) Room-temperature rate capability at different high current rates and (e) cycling at elevated temperatures of 70 °C at 1 C. (a) Reprinted with permission from Ref. [172], Copyright 2018, Elsevier. (b, c) Reprinted with permission from Ref. [121], Copyright 2015, American Chemical Society. (d, e) Reprinted with permission from Ref. [173], Copyright 2019, Elsevier (color online).

with the coating of BN nanosheets and created a more uniform thermal distribution (Figure 14(b, c)). By using BN-coated separators, the Coulombic efficiency maintained at 92% after 100 cycles at 0.5 mA cm^{-2} and 88% after 100 cycles at 1.0 mA cm^{-2}.

Rahman *et al*. [173] synthesized a high-performance inorganic nanomaterial boron nitride nanotube (BNNT) with nanosized diameter along high thermal conductivity. Through double-side coating with BNNTs, the BNNT separator exhibited superior thermal tolerance at the temperature of 150 °C, ensuring the safe operation of LIBs at elevated temperatures. Most importantly, long and fine BNNTs did not block the porous channels of the separators for Li-ion diffusion. The BNNT-coated separator can absorb extra heat and spread it during the cycling process, and thus, the cell with a BNNT separator not only obtained a high reversible capacity at high charge/discharge current rates of 5–10 C, but also operated normally at 50 °C and 70 °C (Figure 14(d, e)). In addition, some researchers have combined BN with other thermal conducting materials to further improve the performance of the separator. Rodriguez *et al*. [170] presented a boron nitride-graphene (BN_xGr_y) layer including layered graphene and BN flakes. Few layered graphene had a thermal conductivity of 1,300 W m^{-1} K^{-1} and a Young's modulus of 20 GPa. The synergistic effect between physicochemical properties of Gr and BN ensured high heat dissipation and mechanical stability of the separator. These properties inhibited the growth of sharp Li dendrites, reduced the polarization and impedance, and significantly improved the performance and stability of Li/Cu semi-batteries (Coulombic efficiency of 83.5% after 100 cycles at 0.5 mA cm^{-2}).

3.4.4 Chemically active separators

During battery cycling, the transition metal (TM) cations' dissolution from oxide materials, shuttle and followed side reactions at both anode and cathode interfaces in LIBs with $LiPF_6$-based electrolytes highly affect the durability and safety of batteries. In addition, the hydrofluoric acid (HF) produced by $LiPF_6$-trace water reactions will promote the dissolution of TM ions. All of these phenomena might accelerate the thermal runaway process of the battery and cause more serious safety problems. In order to prevent the shuttle of TM ions and side reactions between electrodes and electrolytes, researchers conducted extensive studies on different components such as anodes, cathodes, electrolytes and separators [174,175]. In terms of the separator, the chemical active separator with the function of acid-scavenging and trapping TM cations promotes the further research and development of novel separators.

Acid-scavenging separators inhibit the root cause of the dissolution of Mn ions from the positive electrode. Xu *et al*. [176] developed a multifunctional polymer separator coated with Li-zeolite. The coated zeolite could adsorb trace water to reduce the formation of HF and act as HF scavengers to mitigate its attack on the positive electrode. Compared to commercial alumina-coated separators, the cells with lithium-zeolite-coated separators had higher capacities and longer cycle lives at 50 °C, and less transition metal elements were detected on the recycled graphite electrode. Banerjee *et al*. [98] reported a separator coated with a commercial resin, which consisted of a 25% cross-linked divinylbenzene backbone functionalized with 4-vinylpyridine (DVB-4VP). The 4-vinylpyridine functional group prevented acid-induced parasitic reactions by removing acidic protons from the solution phase to reduce parasitic reactions. After cycling at 55 °C for 4 weeks, $LiMn_2O_4$/graphite and $LiNi_{0.6}Mn_{0.2}Co_{0.2}O_2$/graphite cells with functional separators retained higher capacity than the cells with commercial separators.

By means of chelating between TM cations and polymers functionalized with disodium iminodiacetate ($IDANa_2$), PEI, amino-bismethylpyridine (BPA), or tetrasodium ethylenediaminetetracetate (Na_4EDTA) in the chemically active separator can trap TM cations [177,178]. Aurbach's group [177] introduced a commercial resin consisting of iminodiacetic acid disodium salt functional groups on a styrene divinylbenzene polymeric matrix into the commercial separator. $IDANa_2$ achieved chelation through electrostatic interactions with the anionic sites on the chelating functionality. After 100 cycles at C/5 rate, cells with chelate-filled separators retained more than 20% and 55% capacity than the cells with commercial separators at 30 °C and 55 °C, respectively. They also proposed that the introduced macroporous ion chelating resin incorporating electron-donor nitrogen functionalities was effective for capturing TM cations [178]. After cycling at 55 °C, the high-frequency resistance in LMO-graphite cells with functional separators only increased by 10%–40%, which is much lower than that of the plain separator (increased by 80%). Furthermore, the Mn contents in the graphite from cells with poly-BPA or poly-PEI are obviously reduced.

The designed chemically active separators can not only improve the capacity retention, but also further reduce the electrodes' interfacial resistances with the decrease of TM ions damaging the anode surface, which benefits to form a uniform SEI film. The more uniform SEI enables a more homogeneous current distribution, thus avoiding the partial over-charge and over-discharge of the electrode in the process of free discharge, and increasing the durability and safety of the battery [179].

4 Summary and outlooks

Nowadays, LIBs have become one of the most widely used energy storage equipments. However, frequent safety-accidents have caused people to worry about the safety of LIBs. Their safety has become an important factor restricting their developments and applications. As an important part of LIBs, although separators do not participate in the electrolytic reaction, they greatly affect the electrochemical performance and safety of the battery. However, the traditional polyolefin separators cannot meet the increasing market demand due to their poor electrolyte affinity and poor thermal stability. Therefore, developing separators with high thermal stability, high mechanical strength and inhibition of lithium dendrites is an important way to improve the safety of LIBs.

The researchers adopted different modification methods to improve the safety of the separator. For example, in terms of improving the thermal stability, polymeric and inorganic nanoparticles are usually introduced into polyolefin separators, and used to design separators with high heat-resistant skeleton through electrospinning, phase inversion, filtration and other methods. In the aspect of inhibiting the formation of lithium dendrites, lithium-ion nucleation can be promoted, or the uniform transmission of lithium ions can be adjusted by changing the pore size distribution and enhancing the wettability of the separators to reduce the formation of lithium dendrites. In terms of mechanical strength, there are development directions such as dendrite-proof separators, high tensile strength separators and stretchable separators. In addition, for some novel separators, new functions such as flame retardancy, thermal shutdown capacity and high thermal conductivity are introduced to improve the safety of batteries. In a word, for an ideal high-safety separator which meets the basic requirement for fast lithium-ion transport, we hope that it can have the following advantages: (a) high thermal stability and flame retardancy to ensure that the separator can operate stably at elevated temperature; (b) good lithium dendrite resistance which promotes uniform lithium-ion transport and ensures that the battery will not be pierced by lithium dendrites during the cycle, resulting in internal short circuit and potential safety hazard; (c) high mechanical strength which is conducive to the mechanical integrity of the separator during winding and battery assembly; (d) thermal shutdown ability which can timely shut down the battery when it is over-heated to avoid thermal runaway of the battery. However, there is no separator that can fully meet these requirements so far, so it is important to balance these different requirements to achieve the best performance. Therefore, in the future research, we need to make more efforts to improve the overall performance of the separator. Some possible development directions and challenges of battery separators in the future are proposed as below:

(1) Modified polyolefin separators. At present, introducing a coating layer on the polyolefin separator is a commonly used strategy which can improve thermal stability, electrolyte wettability and benefit for large-scale production. However, the weight and the thickness of the modified separators are highly increased to achieve high thermal stability of above 150 °C, which is not conducive to the development of high energy density batteries. Based on this, ultra-thin separators composed of ultra-thin coating layers and thin polyolefin membranes could reduce the weight and occupation of the internal space of the battery, and meet the requirements of high energy density batteries to a certain extent. In addition, with the diversification of the market's requirements for separators, it is imperative to expand new multifunctional modified separators by introducing functional coating layers (such as thermal shutdown, flame retardance, thermal conductivity and dendrite warning functions) on a polyolefin separator to meet the needs of batteries working in different application situations.

(2) High heat-resistant separators. Although introducing

traditional coating layers can improve the thermal stability of polyolefin separators, but limited by the characteristics of polyolefin materials, the modified polyolefin separators are difficult to be stable at higher temperatures (>200 °C). Therefore, high thermal-stable separators with a high heat resistant skeleton have attracted much attention. For example, high heat-resistant polymer nanofiber (PI, PBI, aramid, cellulose, *etc*.) or inorganic metal oxide (Al_2O_3, SiO_2, *etc*.) porous membranes by electrospinning or filtration or other methods could sustain thermal stability at the temperature higher than 200 °C. However, in addition to high production costs, the development of these new types of separators is still limited due to their own defects, such as lack of thermal shutdown function, too high porosity and low mechanical properties which might not be resistant to the lithium dendrite puncture, and low tensile strength which could not meet the requirement of winding operation used during battery assembly. All these disadvantages restrict their large-scale applications in LIBs. Therefore, these problems need to be improved to meet the application requirements of high-safety separators.

(3) Solid-state electrolytes. The solid-state electrolytes with the functions of separators and electrolytes without using the flammable and leaky liquid organic electrolytes have the advantages of high thermal stability, flame retardance, *etc*., which can solve battery safety issues well, and the corresponding solid-state lithium batteries are considered as an ideal power source for high energy density and high-safety energy storage devices [180–182]. In addition, since the solid electrolyte has no flow, solidification and volatilization problems, it can be applied in multiple temperature zones, which broadens the battery's operating temperature range. The widely studied polymer electrolytes are flexible and easy for the large-scale production but still face the problems of low ionic conductivity and poor mechanical strength [183,184]. The inorganic solid-state electrolytes have higher ionic conductivity and mechanical strength, but there is still an urgent need for improving the thin-film fabrication to meet the requirements of practical applications [185–187]. On the other hand, the brittle and mechanical flexibility of inorganic solid-state electrolytes are not conducive to the assembly of solid-state batteries. Therefore, the development of thin solid-state electrolytes with high ionic conductivity and mechanical flexibility is also one of the most important development directions.

Acknowledgements This work was financially supported by the National Key R&D Program of China (2016YFB0100304), the National Natural Science Foundation of China (21776098), Guangdong Natural Science Funds for Distinguished Young Scholar (2017A030306022), the Guangzhou Technology Project (202002030164).

Conflict of interest The authors declare no conflict of interest.

1 Feng X, Ren D, He X, Ouyang M. *Joule*, 2020, 4: 743–770
2 Li Y, Yu L, Hu W, Hu X. *J Mater Chem A*, 2020, 8: 20294–20317
3 Liu X, Ren D, Hsu H, Feng X, Xu GL, Zhuang M, Gao H, Lu L, Han X, Chu Z, Li J, He X, Amine K, Ouyang M. *Joule*, 2018, 2: 2047–2064
4 Lyu P, Liu X, Qu J, Zhao J, Huo Y, Qu Z, Rao Z. *Energy Storage Mater*, 2020, 31: 195–220
5 Deng K, Zeng Q, Wang D, Liu Z, Wang G, Qiu Z, Zhang Y, Xiao M, Meng Y. *Energy Storage Mater*, 2020, 32: 425–447
6 Todorov YM, Aoki M, Mimura H, Fujii K, Yoshimoto N, Morita M. *J Power Sources*, 2016, 332: 322–329
7 Chen Z, Hsu PC, Lopez J, Li Y, To JWF, Liu N, Wang C, Andrews SC, Liu J, Cui Y, Bao Z. *Nat Energy*, 2016, 1: 15009
8 Chen G, Song X, Wang S, Wang Y, Gao T, Ding LX, Wang H. *J Membrane Sci*, 2018, 548: 247–253
9 Song X, Wang S, Chen G, Gao T, Bao Y, Ding LX, Wang H. *Chem Eng J*, 2018, 333: 564–571
10 Song X, Chen G, Wang S, Huang Y, Jiang Z, Ding LX, Wang H. *ACS Appl Mater Interfaces*, 2018, 10: 26274–26282
11 Chen G, Song X, Wang S, Chen X, Wang H. *J Power Sources*, 2018, 408: 58–64
12 Waqas M, Ali S, Feng C, Chen D, Han J, He W. *Small*, 2019, 15: 1901689
13 Lee H, Yanilmaz M, Toprakci O, Fu K, Zhang X. *Energy Environ Sci*, 2014, 7: 3857–3886
14 Zhang C, Li H, Wang S, Cao Y, Yang H, Ai X, Zhong F. *J Energy Chem*, 2020, 44: 33–40
15 Zhao CZ, Chen PY, Zhang R, Chen X, Li BQ, Zhang XQ, Cheng XB, Zhang Q. *Sci Adv*, 2018, 4: eaat3446
16 Li C, Liu S, Shi C, Liang G, Lu Z, Fu R, Wu D. *Nat Commun*, 2019, 10: 1363
17 Dong G, Liu B, Kong L, Wang Y, Tian G, Qi S, Wu D. *ACS Sustain Chem Eng*, 2019, 7: 17643–17652
18 Lagadec MF, Zahn R, Wood V. *Nat Energy*, 2019, 4: 16–25
19 Liang J, Chen Q, Liao X, Yao P, Zhu B, Lv G, Wang X, Chen X, Zhu J. *Angew Chem Int Ed*, 2020, 59: 6561–6566
20 Chen Y, Liu Z, Lin M, Lin Q, Tong B, Chen D. *Sci China Chem*, 2019, 62: 479–490
21 Guan X, Wang A, Liu S, Li G, Liang F, Yang YW, Liu X, Luo J. *Small*, 2018, 14: 1801423
22 Chao CH, Hsieh CT, Ke WJ, Lee LW, Lin YF, Liu HW, Gu S, Fu CC, Juang RS, Mallick BC, Gandomi YA, Su CY. *J Power Sources*, 2021, 482: 228896
23 Zhang W, Tu Z, Qian J, Choudhury S, Archer LA, Lu Y. *Small*, 2018, 14: 1703001
24 Jeon H, Yeon D, Lee T, Park J, Ryou MH, Lee YM. *J Power Sources*, 2016, 315: 161–168
25 Zhang Y, Wang Z, Xiang H, Shi P, Wang H. *J Membrane Sci*, 2016, 509: 19–26
26 Pi JK, Wu GP, Yang HC, Arges CG, Xu ZK. *ACS Appl Mater Interfaces*, 2017, 9: 21971–21978
27 Cho J, Jung YC, Lee YS, Kim DW. *J Membrane Sci*, 2017, 535: 151–157
28 Lei QK, Zhang Q, Wu XY, Wei X, Zhang J, Wang KX, Chen JS. *Chem Eng J*, 2020, 395: 125187
29 Zhang K, Xiao W, Li X, Liu J, Yan C. *J Power Sources*, 2020, 468: 228403
30 Xiang H, Chen J, Li Z, Wang H. *J Power Sources*, 2011, 196: 8651–8655
31 Chen J, Wang S, Cai D, Wang H. *J Membrane Sci*, 2014, 449: 169–175
32 Yang P, Zhang P, Shi C, Chen L, Dai J, Zhao J. *J Membrane Sci*, 2015, 474: 148–155
33 Boateng B, Zhu G, Lv W, Chen D, Feng C, Waqas M, Ali S, Wen K, He W. *Phys Status Solidi RRL*, 2018, 12: 1800319
34 Lee Y, Lee H, Lee T, Ryou MH, Lee YM. *J Power Sources*, 2015,

294: 537–544
35 Shi C, Dai J, Shen X, Peng L, Li C, Wang X, Zhang P, Zhao J. *J Membrane Sci*, 2016, 517: 91–99
36 Dai J, Shi C, Li C, Shen X, Peng L, Wu D, Sun D, Zhang P, Zhao J. *Energy Environ Sci*, 2016, 9: 3252–3261
37 Song Q, Li A, Shi L, Qian C, Feric TG, Fu Y, Zhang H, Li Z, Wang P, Li Z, Zhai H, Wang X, Dontigny M, Zaghib K, Park AHA, Myers K, Chuan X, Yang Y. *Energy Storage Mater*, 2019, 22: 48–56
38 Yang C, Tong H, Luo C, Yuan S, Chen G, Yang Y. *J Power Sources*, 2017, 348: 80–86
39 Zheng H, Wang Z, Shi L, Zhao Y, Yuan S. *J Colloid Interface Sci*, 2019, 554: 29–38
40 Waqas M, Tan C, Lv W, Ali S, Boateng B, Chen W, Wei Z, Feng C, Ahmed J, Goodenough JB, He W. *ChemElectroChem*, 2018, 5: 2722–2728
41 Waqas M, Ali S, Lv W, Chen D, Boateng B, He W. *Adv Mater Interfaces*, 2019, 6: 1801330
42 Zhang SS, Fan X, Wang C. *J Mater Chem A*, 2018, 6: 10755–10760
43 Liao C, Wang W, Han L, Mu X, Wu N, Wang J, Gui Z, Hu Y, Kan Y, Song L. *Appl Mater Today*, 2020, 21: 100793
44 Shi C, Zhang P, Chen L, Yang P, Zhao J. *J Power Sources*, 2014, 270: 547–553
45 Zhang P, Chen L, Shi C, Yang P, Zhao J. *J Power Sources*, 2015, 284: 10–15
46 Yang Y, Wang W, Zhang J. *Mater Today Energy*, 2020, 16: 100420
47 Wang X, Peng L, Hua H, Liu Y, Zhang P, Zhao J. *ChemElectroChem*, 2020, 7: 1187–1192
48 Qiu Z, Yuan S, Wang Z, Shi L, Jo JH, Myung ST, Zhu J. *J Power Sources*, 2020, 472: 228445
49 Zhu X, Jiang X, Ai X, Yang H, Cao Y. *J Membrane Sci*, 2016, 504: 97–103
50 Jiang X, Zhu X, Ai X, Yang H, Cao Y. *ACS Appl Mater Interfaces*, 2017, 9: 25970–25975
51 Han M, Kim DW, Kim YC. *ACS Appl Mater Interfaces*, 2016, 8: 26073–26081
52 Chi M, Shi L, Wang Z, Zhu J, Mao X, Zhao Y, Zhang M, Sun L, Yuan S. *Nano Energy*, 2016, 28: 1–11
53 Pan R, Sun R, Wang Z, Lindh J, Edström K, Strømme M, Nyholm L. *Nano Energy*, 2019, 55: 316–326
54 Moon J, Jeong JY, Kim JI, Kim S, Park JH. *J Power Sources*, 2019, 416: 89–94
55 Pan R, Xu X, Sun R, Wang Z, Lindh J, Edström K, Strømme M, Nyholm L. *Small*, 2018, 14: 1704371
56 Yang SY, Rubner MF. *J Am Chem Soc*, 2002, 124: 2100–2101
57 Kim BS, Park SW, Hammond PT. *ACS Nano*, 2008, 2: 386–392
58 Jin R, Fu L, Zhou H, Wang Z, Qiu Z, Shi L, Zhu J, Yuan S. *ACS Sustain Chem Eng*, 2018, 6: 2961–2968
59 Na W, Koh KH, Lee AS, Cho S, Ok B, Hwang SW, Lee JH, Koo CM. *J Membrane Sci*, 2019, 573: 621–627
60 Zhu C, Nagaishi T, Shi J, Lee H, Wong PY, Sui J, Hyodo K, Kim IS. *ACS Appl Mater Interfaces*, 2017, 9: 26400–26406
61 Zhang J, Xiang Y, Jamil MI, Lu J, Zhang Q, Zhan X, Chen F. *J Membrane Sci*, 2018, 564: 753–761
62 Yanilmaz M, Lu Y, Zhu J, Zhang X. *J Power Sources*, 2016, 313: 205–212
63 Hu S, Lin S, Tu Y, Hu J, Wu Y, Liu G, Li F, Yu F, Jiang T. *J Mater Chem A*, 2016, 4: 3513–3526
64 He L, Qiu T, Xie C, Tuo X. *J Appl Polym Sci*, 2018, 135: 46697
65 Liu X, Song K, Lu C, Huang Y, Duan X, Li S, Ding Y. *J Membrane Sci*, 2018, 555: 1–6
66 Asghar MR, Zhang Y, Wu A, Yan X, Shen S, Ke C, Zhang J. *J Power Sources*, 2018, 379: 197–205
67 Huang F, Xu Y, Peng B, Su Y, Jiang F, Hsieh YL, Wei Q. *ACS Sustain Chem Eng*, 2015, 3: 932–940
68 Zhang B, Wang Q, Zhang J, Ding G, Xu G, Liu Z, Cui G. *Nano Energy*, 2014, 10: 277–287
69 Zhao H, Deng N, Wang G, Ren H, Kang W, Cheng B. *Chem Eng J*, 2021, 404: 126542
70 Hao X, Zhu J, Jiang X, Wu H, Qiao J, Sun W, Wang Z, Sun K. *Nano Lett*, 2016, 16: 2981–2987
71 Chen J, Wang S, Ding L, Jiang Y, Wang H. *J Membrane Sci*, 2014, 461: 22–27
72 Li Y, Li Q, Tan Z. *J Power Sources*, 2019, 443: 227262
73 Lin CE, Zhang H, Song YZ, Zhang Y, Yuan JJ, Zhu BK. *J Mater Chem A*, 2018, 6: 991–998
74 Sun G, Kong L, Liu B, Niu H, Zhang M, Tian G, Qi S, Wu D. *J Membrane Sci*, 2019, 582: 132–139
75 Li H, Zhang B, Lin B, Yang Y, Zhao Y, Wang L. *J Electrochem Soc*, 2018, 165: A939–A946
76 Hao J, Lei G, Li Z, Wu L, Xiao Q, Wang L. *J Membrane Sci*, 2013, 428: 11–16
77 Li D, Shi D, Feng K, Li X, Zhang H. *J Membrane Sci*, 2017, 530: 125–131
78 Kong L, Yan Y, Qiu Z, Zhou Z, Hu J. *J Membrane Sci*, 2018, 549: 321–331
79 Kong L, Liu B, Ding J, Yan X, Tian G, Qi S, Wu D. *J Membrane Sci*, 2018, 549: 244–250
80 Jung JW, Lee CL, Yu S, Kim ID. *J Mater Chem A*, 2016, 4: 703–750
81 Wang Y, Wang S, Fang J, Ding LX, Wang H. *J Membrane Sci*, 2017, 537: 248–254
82 Zhao H, Deng N, Yan J, Kang W, Ju J, Wang L, Li Z, Cheng B. *Chem Eng J*, 2019, 356: 11–21
83 Shi C, Dai J, Huang S, Li C, Shen X, Zhang P, Wu D, Sun D, Zhao J. *J Membrane Sci*, 2016, 518: 168–177
84 Yang S, Ma W, Wang A, Gu J, Yin Y. *RSC Adv*, 2018, 8: 23390–23396
85 Wang L, Deng N, Ju J, Wang G, Cheng B, Kang W. *Electrochim Acta*, 2019, 300: 263–273
86 Du QC, Yang MT, Yang JK, Zhang P, Qi JQ, Bai L, Li Z, Chen JY, Liu RQ, Feng XM, Huang ZD, Masese T, Ma YW, Huang W. *ACS Appl Mater Interfaces*, 2019, 11: 34895–34903
87 Sheng J, Chen T, Wang R, Zhang Z, Hua F, Yang R. *J Membrane Sci*, 2020, 595: 117550
88 Lu W, Yuan Z, Zhao Y, Zhang H, Zhang H, Li X. *Chem Soc Rev*, 2017, 46: 2199–2236
89 He M, Zhang X, Jiang K, Wang J, Wang Y. *ACS Appl Mater Interfaces*, 2015, 7: 738–742
90 Zhang T, Chen J, Tian T, Shen B, Peng Y, Song Y, Jiang B, Lu L, Yao H, Yu S. *Adv Funct Mater*, 2019, 29: 1902023
91 Liang Y, Cheng S, Zhao J, Zhang C, Sun S, Zhou N, Qiu Y, Zhang X. *J Power Sources*, 2013, 240: 204–211
92 Carol P, Ramakrishnan P, John B, Cheruvally G. *J Power Sources*, 2011, 196: 10156–10162
93 Chen W, Liu Y, Ma Y, Yang W. *J Power Sources*, 2015, 273: 1127–1135
94 Zhai Y, Xiao K, Yu J, Yang J, Ding B. *J Mater Chem A*, 2015, 3: 10551–10558
95 Jiang Y, Ding Y, Zhang P, Li F, Yang Z. *J Membrane Sci*, 2018, 565: 33–41
96 Zhang C, Shen L, Shen J, Liu F, Chen G, Tao R, Ma S, Peng Y, Lu Y. *Adv Mater*, 2019, 31: 1808338
97 de Moraes ACM, Hyun WJ, Luu NS, Lim JM, Park KY, Hersam MC. *ACS Appl Mater Interfaces*, 2020, 12: 8107–8114
98 Banerjee A, Ziv B, Shilina Y, Luski S, Aurbach D, Halalay IC. *ACS Energy Lett*, 2017, 2: 2388–2393
99 Wang M, Chen X, Wang H, Wu H, Jin X, Huang C. *J Mater Chem A*, 2017, 5: 311–318
100 Zhang J, Zhu C, Xu J, Wu J, Yin X, Chen S, Zhu Z, Wang L, Li ZC. *J Membrane Sci*, 2020, 597: 117622
101 Li Q, Tan S, Li L, Lu Y, He Y. *Sci Adv*, 2017, 3: e1701246
102 Xu K. *Chem Rev*, 2004, 104: 4303–4418
103 Wang C, Wang A, Ren L, Guan X, Wang D, Dong A, Zhang C, Li G, Luo J. *Adv Funct Mater*, 2019, 29: 1905940
104 Xie H, Hao Q, Jin H, Xie S, Sun Z, Ye Y, Zhang C, Wang D, Ji H,

Wan LJ. *Sci China Chem*, 2020, 63: 1306–1314
105 Zhao J, Chen D, Boateng B, Zeng G, Han Y, Zhen C, Goodenough JB, He W. *J Power Sources*, 2020, 451: 227773
106 Rao Z, Yang Z, Gong W, Su S, Fu Q, Huang Y. *J Mater Chem A*, 2020, 8: 3859–3864
107 Yang J, Wang CY, Wang CC, Chen KH, Mou CY, Wu HL. *J Mater Chem A*, 2020, 8: 5095–5104
108 Zhang SS. *J Power Sources*, 2007, 164: 351–364
109 Ryou MH, Lee DJ, Lee JN, Lee YM, Park JK, Choi JW. *Adv Energy Mater*, 2012, 2: 645–650
110 Wang Y, Shi L, Zhou H, Wang Z, Li R, Zhu J, Qiu Z, Zhao Y, Zhang M, Yuan S. *Electrochim Acta*, 2018, 259: 386–394
111 Chen W, Shi L, Wang Z, Zhu J, Yang H, Mao X, Chi M, Sun L, Yuan S. *Carbohydrate Polyms*, 2016, 147: 517–524
112 Huo H, Li X, Chen Y, Liang J, Deng S, Gao X, Doyle-Davis K, Li R, Guo X, Shen Y, Nan CW, Sun X. *Energy Storage Mater*, 2020, 29: 361–366
113 Xu Y, Zhou Y, Li T, Jiang S, Qian X, Yue Q, Kang Y. *Energy Storage Mater*, 2020, 25: 334–341
114 Boriboon D, Vongsetskul T, Limthongkul P, Kobsiriphat W, Tammawat P. *Carbohydrate Polyms*, 2018, 189: 145–151
115 Liu W, Mi Y, Weng Z, Zhong Y, Wu Z, Wang H. *Chem Sci*, 2017, 8: 4285–4291
116 Wang Z, Huang W, Hua J, Wang Y, Yi H, Zhao W, Zhao Q, Jia H, Fei B, Pan F. *Small Methods*, 2020, 4: 2000082
117 Shen L, Wu HB, Liu F, Zhang C, Ma S, Le Z, Lu Y. *Nanoscale Horiz*, 2019, 4: 705–711
118 Chen C, Zhang W, Zhu H, Li BG, Lu Y, Zhu S. *Nano Res*, 2020, 14: 1465–1470
119 Panda DK, Maity K, Palukoshka A, Ibrahim F, Saha S. *ACS Sustain Chem Eng*, 2019, 7: 4619–4624
120 Zhu Y, Xie J, Pei A, Liu B, Wu Y, Lin D, Li J, Wang H, Chen H, Xu J, Yang A, Wu CL, Wang H, Chen W, Cui Y. *Nat Commun*, 2019, 10: 2067
121 Luo W, Zhou L, Fu K, Yang Z, Wan J, Manno M, Yao Y, Zhu H, Yang B, Hu L. *Nano Lett*, 2015, 15: 6149–6154
122 Li X, Liu Y, Pan Y, Wang M, Chen J, Xu H, Huang Y, Lau WM, Shan A, Zheng J, Mitlin D. *J Mater Chem A*, 2019, 7: 21349–21361
123 Hu Z, Liu F, Gao J, Zhou W, Huo H, Zhou J, Li L. *Adv Funct Mater*, 2020, 30: 1907020
124 Boateng B, Han Y, Zhen C, Zeng G, Chen N, Chen D, Feng C, Han J, Xiong J, Duan X, He W. *Nano Lett*, 2020, 20: 2594–2601
125 Yan J, Liu F, Hu Z, Gao J, Zhou W, Huo H, Zhou J, Li L. *Nano Lett*, 2020, 20: 3798–3807
126 Zhou D, Liu R, He YB, Li F, Liu M, Li B, Yang QH, Cai Q, Kang F. *Adv Energy Mater*, 2016, 6: 1502214
127 Fu S, Wang L, Zhao T, Li L, Wu F, Chen R. *ChemElectroChem*, 2020, 7: 2159–2164
128 Ye M, Xiao Y, Cheng Z, Cui L, Jiang L, Qu L. *Nano Energy*, 2018, 49: 403–410
129 Liu K, Zhuo D, Lee HW, Liu W, Lin D, Lu Y, Cui Y. *Adv Mater*, 2017, 29: 1603987
130 Chen X, Zhang R, Zhao R, Qi X, Li K, Sun Q, Ma M, Qie L, Huang Y. *Energy Storage Mater*, 2020, 31: 181–186
131 Tung SO, Ho S, Yang M, Zhang R, Kotov NA. *Nat Commun*, 2015, 6: 6152
132 Liu J, Mo Y, Wang S, Ren S, Han D, Xiao M, Sun L, Meng Y. *ACS Appl Energy Mater*, 2019, 2: 3886–3895
133 Blin P, Boury B, Taguet A, Touja J, Monconduit L, Patra S. *Carbohydrate Polyms*, 2020, 247: 116697
134 Na W, Lee AS, Lee JH, Hwang SS, Kim E, Hong SM, Koo CM. *ACS Appl Mater Interfaces*, 2016, 8: 12852–12858
135 Wang W, Liao C, Liew KM, Chen Z, Song L, Kan Y, Hu Y. *J Mater Chem A*, 2019, 7: 6859–6868
136 Ansari Y, Guo B, Cho JH, Park K, Song J, Ellison CJ, Goodenough JB. *J Electrochem Soc*, 2014, 161: A1655–A1661
137 Tu Z, Kambe Y, Lu Y, Archer LA. *Adv Energy Mater*, 2014, 4: 1300654
138 Liu L, Xu T, Gui X, Gao S, Sun L, Lin Q, Song X, Wang Z, Xu K. *Compos Part B-Eng*, 2021, 215: 108849
139 Dong G, Dong N, Liu B, Tian G, Qi S, Wu D. *J Membrane Sci*, 2020, 601: 117884
140 Kong L, Wang Y, Yu H, Liu BX, Qi S, Wu D, Zhong WH, Tian G, Wang J. *ACS Appl Mater Interfaces*, 2019, 11: 2978–2988
141 Sun G, Dong G, Kong L, Yan X, Tian G, Qi S, Wu D. *Nanoscale*, 2018, 10: 22439–22447
142 Patel A, Wilcox K, Li Z, George I, Juneja R, Lollar C, Lazar S, Grunlan J, Tenhaeff WE, Lutkenhaus JL. *ACS Appl Mater Interfaces*, 2020, 12: 25756–25766
143 Liu J, Yang K, Mo Y, Wang S, Han D, Xiao M, Meng Y. *J Power Sources*, 2018, 400: 502–510
144 Mackanic DG, Kao M, Bao Z. *Adv Energy Mater*, 2020, 10: 2001424
145 Li H, Wu D, Wu J, Dong LY, Zhu YJ, Hu X. *Adv Mater*, 2017, 29: 1703548
146 Shin M, Song WJ, Son HB, Yoo S, Kim S, Song G, Choi NS, Park S. *Adv Energy Mater*, 2018, 8: 1801025
147 Liu W, Chen J, Chen Z, Liu K, Zhou G, Sun Y, Song MS, Bao Z, Cui Y. *Adv Energy Mater*, 2017, 7: 1701076
148 Jansen AN, Kahaian AJ, Kepler KD, Nelson PA, Amine K, Dees DW, Vissers DR, Thackeray MM. *J Power Sources*, 1999, 81-82: 902–905
149 Walton JJ, Hiasa T, Kumita H, Takeshi K, Sandford G. *ACS Appl Mater Interfaces*, 2020, 12: 15893–15902
150 Xie Y, Zou H, Xiang H, Xia R, Liang D, Shi P, Dai S, Wang H. *J Membrane Sci*, 2016, 503: 25–30
151 Xie Y, Xiang H, Shi P, Guo J, Wang H. *J Membrane Sci*, 2017, 524: 315–320
152 Yamada Y, Furukawa K, Sodeyama K, Kikuchi K, Yaegashi M, Tateyama Y, Yamada A. *J Am Chem Soc*, 2014, 136: 5039–5046
153 Wang J, Yamada Y, Sodeyama K, Chiang CH, Tateyama Y, Yamada A. *Nat Commun*, 2016, 7: 12032
154 Chen Y, Qiu L, Ma X, Dong L, Jin Z, Xia G, Du P, Xiong J. *Carbohydrate Polyms*, 2020, 234: 115907
155 Yim T, Park MS, Woo SG, Kwon HK, Yoo JK, Jung YS, Kim KJ, Yu JS, Kim YJ. *Nano Lett*, 2015, 15: 5059–5067
156 Zhu C, Zhang J, Xu J, Yin X, Wu J, Chen S, Zhu Z, Wang L, Wang H. *J Membrane Sci*, 2019, 588: 117169
157 Liu K, Liu W, Qiu Y, Kong B, Sun Y, Chen Z, Zhuo D, Lin D, Cui Y. *Sci Adv*, 2017, 3: e1601978
158 Peng L, Kong X, Li H, Wang X, Shi C, Hu T, Liu Y, Zhang P, Zhao J. *Adv Funct Mater*, 2021, 31: 2008537
159 Jing P, Liu M, Wang P, Yang J, Tang M, He C, Pu Y, Liu M. *Chem Eng J*, 2020, 388: 124259
160 Venugopal G, Moore J, Howard J, Pendalwar S. *J Power Sources*, 1999, 77: 34–41
161 Li Y, Pu H, Wei Y. *Electrochim Acta*, 2018, 264: 140–149
162 Liu J, Liu Y, Yang W, Ren Q, Li F, Huang Z. *J Power Sources*, 2018, 396: 265–275
163 Pitchan MK, Bhowmik S, Balachandran M, Abraham M. *Mater Des*, 2017, 127: 193–203
164 Li D, Shi D, Yuan Z, Feng K, Zhang H, Li X. *J Membrane Sci*, 2017, 542: 1–7
165 Sun G, Liu B, Niu H, Hao F, Chen N, Zhang M, Tian G, Qi S, Wu D. *J Membrane Sci*, 2020, 595: 117509
166 Li Z, Xiong Y, Sun S, Zhang L, Li S, Liu X, Xu Z, Xu S. *J Membrane Sci*, 2018, 565: 50–60
167 Shi C, Zhang P, Huang S, He X, Yang P, Wu D, Sun D, Zhao J. *J Power Sources*, 2015, 298: 158–165
168 Baginska M, Blaiszik BJ, Merriman RJ, Sottos NR, Moore JS, White SR. *Adv Energy Mater*, 2012, 2: 583–590
169 Jiang X, Xiao L, Ai X, Yang H, Cao Y. *J Mater Chem A*, 2017, 5: 23238–23242
170 Rodriguez JR, Kim PJ, Kim K, Qi Z, Wang H, Pol VG. *J Colloid Interface Sci*, 2021, 583: 362–370

171 Shim J, Kim HJ, Kim BG, Kim YS, Kim DG, Lee JC. *Energy Environ Sci*, 2017, 10: 1911–1916
172 Liu Y, Qiao Y, Zhang Y, Yang Z, Gao T, Kirsch D, Liu B, Song J, Yang B, Hu L. *Energy Storage Mater*, 2018, 12: 197–203
173 Rahman MM, Mateti S, Cai Q, Sultana I, Fan Y, Wang X, Hou C, Chen Y. *Energy Storage Mater*, 2019, 19: 352–359
174 Banerjee A, Shilina Y, Ziv B, Ziegelbauer JM, Luski S, Aurbach D, Halalay IC. *J Electrochem Soc*, 2017, 164: A6315–A6323
175 Banerjee A, Ziv B, Shilina Y, Ziegelbauer JM, Liu H, Harris KJ, Botton G, Goward GR, Luski S, Aurbach D, Halalay IC. *J Electrochem Soc*, 2019, 166: A5369–A5377
176 Xu J, Xiao X, Zeng S, Cai M, Verbrugge MW. *ACS Appl Energy Mater*, 2018, 1: 7237–7243
177 Banerjee A, Ziv B, Shilina Y, Luski S, Aurbach D, Halalay IC. *J Electrochem Soc*, 2016, 163: A1083–A1094
178 Banerjee A, Ziv B, Luski S, Aurbach D, Halalay IC. *J Power Sources*, 2017, 341: 457–465
179 Liu H, Banerjee A, Ziv B, Harris KJ, Pieczonka NPW, Luski S, Botton GA, Goward GR, Aurbach D, Halalay IC. *ACS Appl Energy Mater*, 2018, 1: 1878–1882
180 Jiang Z, Xie H, Wang S, Song X, Yao X, Wang H. *Adv Energy Mater*, 2018, 8: 1801433
181 Kaup K, Bazak JD, Vajargah SH, Wu X, Kulisch J, Goward GR, Nazar LF. *Adv Energy Mater*, 2020, 10: 1902783
182 Chen X, He W, Ding LX, Wang S, Wang H. *Energy Environ Sci*, 2019, 12: 938–944
183 Liu C, Wang J, Kou W, Yang Z, Zhai P, Liu Y, Wu W, Wang J. *Chem Eng J*, 2021, 404: 126517
184 Han Q, Wang S, Jiang Z, Hu X, Wang H. *ACS Appl Mater Interfaces*, 2020, 12: 20514–20521
185 Jiang Z, Wang S, Chen X, Yang W, Yao X, Hu X, Han Q, Wang H. *Adv Mater*, 2020, 32: 1906221
186 Wu W, Duan J, Wen J, Chen Y, Liu X, Huang L, Wang Z, Deng S, Huang Y, Luo W. *Sci China Chem*, 2020, 63: 1483–1489
187 Zhao CZ, Duan H, Huang JQ, Zhang J, Zhang Q, Guo YG, Wan LJ. *Sci China Chem*, 2019, 62: 1286–1299